

**KfK 3866
CNEN 1101
Januar 1985**

Radon Measurements in Mines and Dwellings

**M. Urban
Hauptabteilung Sicherheit
D. A. C. Binns, J. J. Estrada
Instituto de Radioproteção e Dosimetria, CNEN**

Kernforschungszentrum Karlsruhe

KERNFORSCHUNGSZENTRUM KARLSRUHE
Hauptabteilung Sicherheit

KfK 3866

CNEN 1101

RADON MEASUREMENTS IN MINES AND DWELLINGS

M. Urban, D.A.C. Binns⁺), J.J. Estrada⁺)

⁺) Instituto de Radioproteção e Dosimetria
Comissão Nacional de Energia Nuclear
Rio de Janeiro, República Federativa do Brasil

Als Manuskript vervielfältigt
Für diesen Bericht behalten wir uns alle Rechte vor

Kernforschungszentrum Karlsruhe GmbH
ISSN 0303-4003

PREFACE

The Federative Republic of Brazil and the Federal Republic of Germany signed an Agreement of Nuclear Cooperation in 1975. Within the framework of this accord, a special agreement providing for scientific and technical cooperation between the Brazilian National Nuclear Energy Commission (CNEN) and the Karlsruhe Nuclear Research Center (KfK) was signed on March 8, 1978. The exchange of scientists and researchers that ensued between the Institute for Radioprotection and Dosimetry of CNEN and the Central Safety Department of KfK led to programs of cooperation in environmental monitoring at nuclear facilities. This cooperation has been extended to include surveys of occupational and environmental exposures due to radon.

The joint program on radon monitoring was started in 1982, at a time when the German national radon survey program was already underway. The first objective of the joint program was to test the dosimeter used in Germany under the very different exposure conditions in an open pit uranium mine in a tropical region. Therefore, a pilot study was performed in the mine of Poços de Caldas. To compare with findings in the Federal Republic of Germany, some additional measurements were conducted in dwellings in Brazil.

The exchange of data and experience within this program was very important to both institutes. This joint report outlines the state of the art of measuring technique and some first results of the pilot study. In addition, a review is presented of radon exposure calculations and dose estimates in uranium mines and private homes.

On behalf of CNEN and KfK we take great pleasure in presenting this joint report on the results of radon measurements. The program and this report constitute an excellent example of successful international cooperation.

Dr. Carlos Eduardo V. de Almeida

Dipl.-Phys. Winfried Koelzer

Director of the Institute for
Radioprotection and Dosimetry,
Federative Republic of Brazil

Head of the Central Safety Department,
Karlsruhe Nuclear Research Center,
Federal Republic of Germany

Rio de Janeiro, January 1985

Karlsruhe, January 1985

ABSTRACT

Radon measurements using a time integrating passive radon dosimeter have been performed in Brazilian and German mines and dwellings. The present state of the measurement technique is summarized. The results are presented together with exposure calculations and dose estimations for occupational exposure in open pit and underground mines and for the general public in houses.

Radonmessungen in Bergwerken und in Wohnhäusern**ZUSAMMENFASSUNG**

Mit Hilfe eines passiven, zeitlich integrierenden Radondosimeters wurden Messungen in brasilianischen und deutschen Bergwerken und in Wohnhäusern durchgeführt. Der Bericht beschreibt den derzeitigen Stand der technischen Entwicklung des Meßverfahrens. Die ersten Ergebnisse werden vorgestellt. Es werden Dosisabschätzungen für die beruflich exponierten Bergarbeiter und die Bevölkerung in Wohnhäusern durchgeführt.

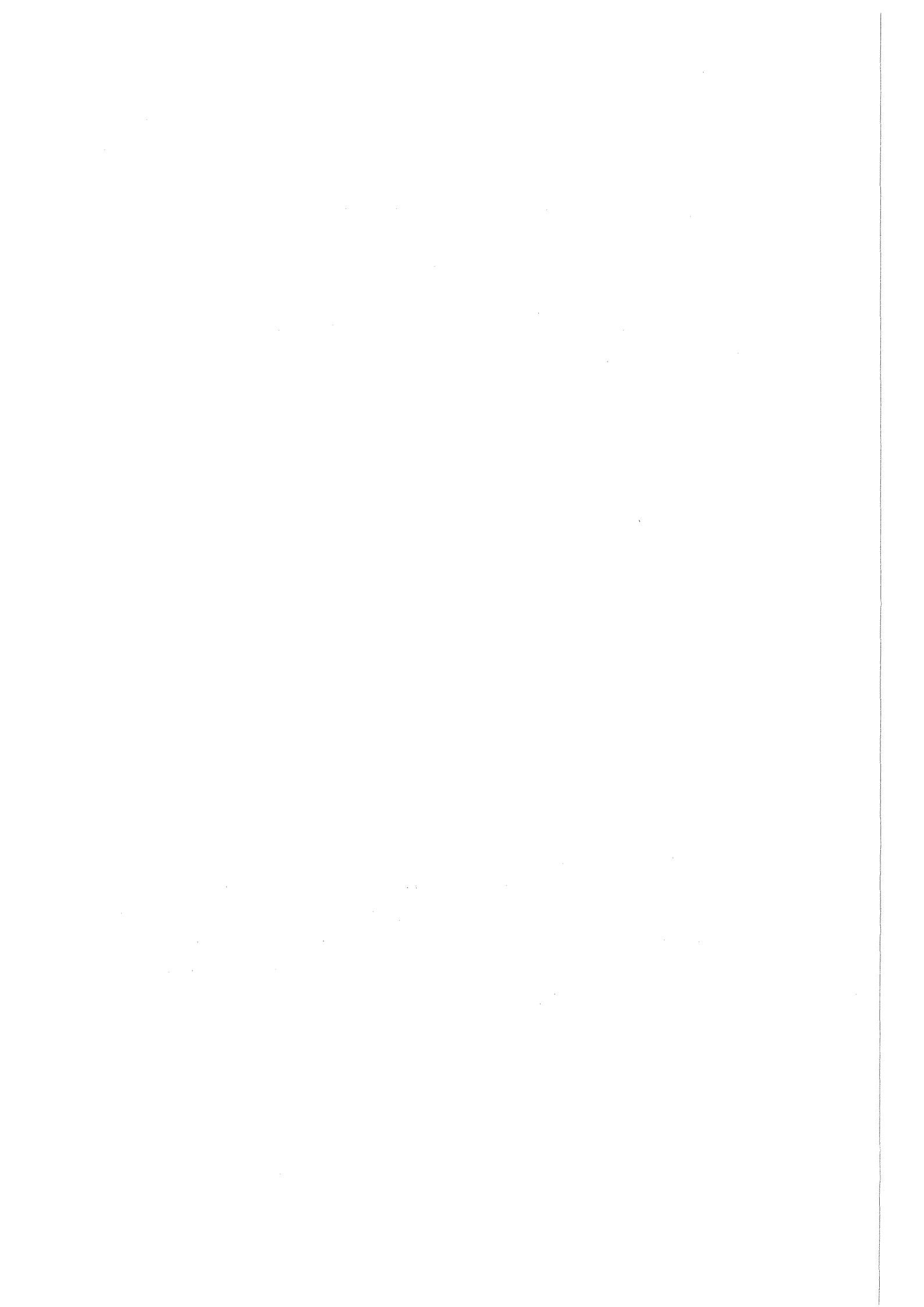


Table of Contents		page
1.	INTRODUCTION	1
2.	MEASUREMENT TECHNIQUES	2
2.1	Selection of a suitable detector material	7
2.2	Processing of the MAKROFOL track etch detectors	7
2.2.1	Electrochemical etching	7
2.2.2	Etching system for processing large series of detectors	10
2.2.3	Counting of tracks	13
2.3	Calculation of the mean radon concentration	15
2.3.1	Radon exposure	15
2.3.2	Uncertainty of radon measurements	18
2.4	Reproducibility	20
2.5	Fading of the track etch detectors	20
3.	MEASUREMENTS IN MINES	23
3.1	Brazilian mines	23
3.2	Monitoring in German mines and mining areas	23
3.2.1	Environmental monitoring	23
3.2.2	Monitoring in mines	27
3.2.3	Personal dosimetry	29
4.	MEASUREMENTS IN HOUSES	29
4.1	Brazilian houses	29
4.2	German houses	34
4.2.1	The German national survey	34
4.2.2	Radon concentration in outside air	36
4.2.3	Radon concentration in houses influenced by geology	41
4.2.4	Radon concentration in houses influenced by mining activities	44

IV

	page
5. EXPOSURE AND DOSE ESTIMATION	48
5.1 Inhalation of radon and short lived decay products	48
5.2 Exposure and dose calculation	49
5.2.1 Equilibrium factor	49
5.2.2 Occupancy factor	50
5.2.3 Exposure calculation	53
5.3 Dose estimation	56
6. REFERENCES	60
7. APPENDIX	63

1. INTRODUCTION

Apart from chemical agents, radioactivity is a contributor to atmospheric pollution. The importance of airborne radioactivity from the health point of view is mainly due to the possibility of incorporating the radioactive contaminant by inhalation.

Nuclear explosions have contributed to the global radioactivity in the atmosphere. Today, the use of nuclear energy for peaceful purposes may involve operations releasing radioactivity to the atmosphere. Reactors and fuel processing plants are among the many sources of airborne contamination which can affect the general public and much engineering effort is devoted to safety considerations of such facilities in order to reduce the probability of exposure of the public.

One dominant and almost inevitable source of airborne radioactivity is natural radioactivity. The major process by which natural radioactivity is released into the atmosphere is the emanation from the ground of the noble gases radon (Rn-222) and thoron (Rn-220), which are produced as a result of the decay of radium and thorium in the earth's crust. As radon and thoron decay in the atmosphere, their daughter products, which are isotopes of the heavy metals polonium, lead and bismuth are created in the atmosphere.

The content of Rn-222 and decay products in air depends on the radium content in the upper ground layer, and on petrological, meteorological and geological conditions. Their concentrations in air therefore change with time and places. Average values for Rn-222 in free air near the ground level in continental regions are in the range of 1 - 10 Bq/m³ (UN 82).

The radon concentration inside houses depends on the radon influx from the ground, the radium content of the walls and the ventilation rate of the room. In normal, naturally ventilated rooms with stone walls the radon concentration is expected to be about a factor of 2 to 5 higher than in free air near ground level.

Since radon and daughter products in indoor air are supposed to be the most important source of natural radiation exposure to the population more information about radon concentration levels seems to be necessary.

The radioactive climate in a uranium mine and its environment is very complex. In addition to the direct radiation exposure from the ore and the host rock, the exposure by the air path i. e. by ore dust and radon and its daughters is of severe importance. This should be considered not only for the employees of the mine or mill site but as well for the public living in the neighborhood of these installations (Sc 83).

While for the dosimetry of the external radiation the instrumentation is well approved to a high standard, the measurement of internal exposure by radon and its daughters is relative laborious and unprecise. There are several instruments available for grab sampling and continuous monitoring of radon and its daughters in mines and in the environment. Best estimation of exposure, however, is done by integrating measuring equipment and integrating personal dosimeters. They especially in the field of environmental monitoring exclude the difficulties with momentary radon concentrations, which may arise due to variations in concentration of an order of magnitude or more during a day.

2. MEASUREMENT TECHNIQUES

There are two different techniques used today for radon measurements, active and passive systems. Active techniques need an external power supply for pumps and electronics. Passive devices do not need such a power supply. They use thermoluminescent detectors (TLD) such as $\text{CaSO}_4:\text{Dy}$ or LiF or track etch detectors as cellulose nitrate, polycarbonate or CR 39. More detailed information is available from literature (Ur 81, Wi 83).

Radon doseimeters making use of a passive alpha detector are constructed in three different ways:

- Active devices with an air gas flow where radon daughters are collected on a filter in front of the detector.
- Passive devices without gas flow in which radon diffuses in a closed chamber and in which alpha particles from radon and daughters from a given air volume or after plate-out from a chamber surface are detected.
- Passive devices using a bare detector which registers radon and daughter products in the ambient air.

For the purpose of this report the diffusion chamber developed at the Karlsruhe Nuclear Research Center was used (Ur 81). The design of the diffusion chamber and the cross section are shown in Fig. 2.1 and Fig. 2.2.

The diffusion chamber contains one detector foil at the bottom. It is closed by a hydrophobic fiberglas filter. A special cover on the chamber avoids contamination by large dust particles on the filter. The design of the chamber ensures that all aerosols and radon decay products are deposited on the filter and that only radon and thoron diffuse through the filter into the sensitive volume of the chamber. The detector foil is located in the conical shaped wall of the chamber in special recesses. The cover of the chamber holds a plastic ring and the filter. The chamber is made from LURAN S, produced by BASF, Ludwigshafen, as a pressure decasting.

The cross section in Fig. 2.3 shows the sensitive volumes and areas of the diffusion chamber. The range of alpha-particles presented in Fig. 2.3 corresponds to the energy range $0.5 < E < 2$ MeV, emitted from Rn-222, Po-218 and Po-214 and registered in the detector. Radon alpha-decays from a small volume element at a short distance from the detector foil are detected. The main contribution to alpha-particles comes from Po-214 attached to a relative large surface, principally at the front of the detector foil, and to Po-218 plated out on a small surface ring in the chamber.

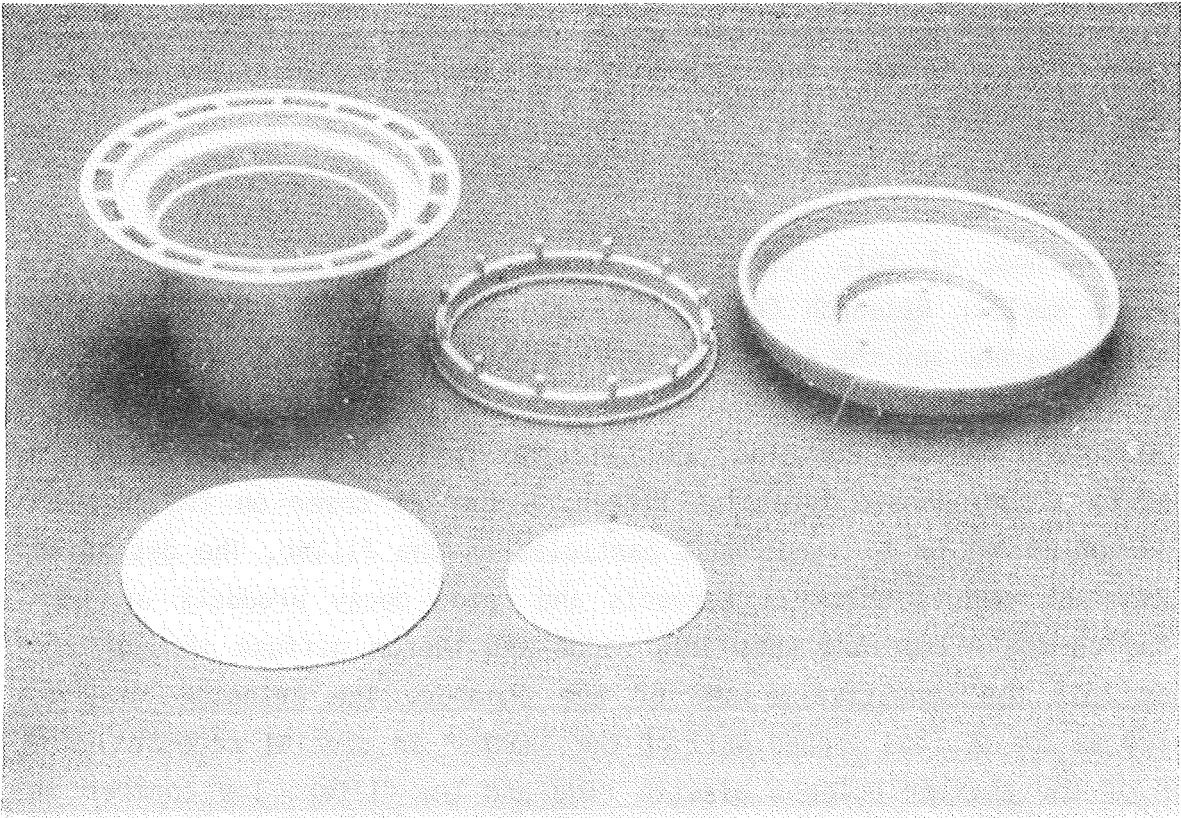


Fig. 2.1: KfK Radon Diffusion Chamber.

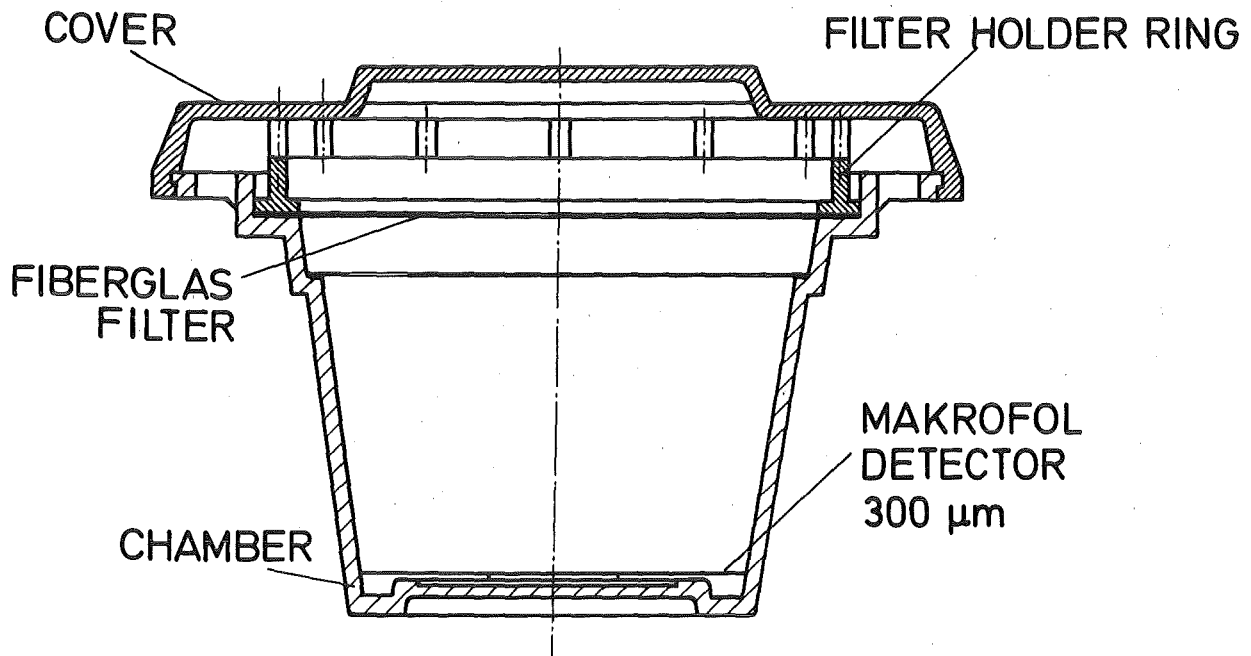


Fig. 2.2: Cross section of the KfK Diffusion Chamber.

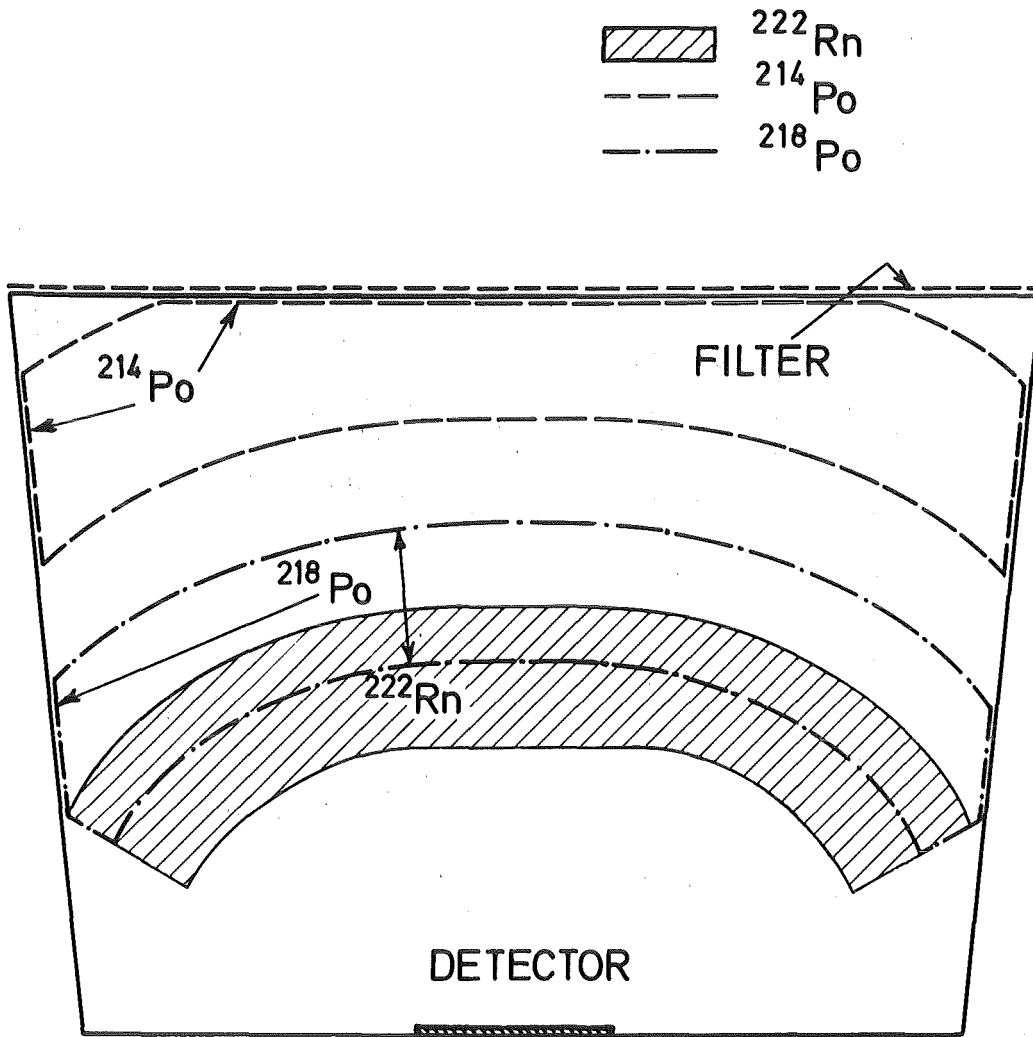


Fig. 2.3: Cross section of the diffusion chamber with the range of alpha particles of Rn-222, Po-218 and Po-214.

2.1 Selection of a suitable detector material

For detection of alpha-particles TLD and track etch detectors can be used. The main disadvantage for TLDs is the low sensitivity for alpha particles compared to the sensitivity to beta and gamma rays. To determine the number of alpha particles a second shielded TLD is necessary. The difference of both readings is related to the wanted number of alpha particles.

At this time there are about 150 different track etch detector materials known (F1 75). The most common of these are cellulose nitrate, polycarbonate and alyldiglycolcarbonate. The best sensitivity so far known is for CR 39. For radon dosimetry mostly CR 39, LR 115, MAKROFOL and LEXAN are used. These materials are insensitive to beta and gamma rays.

In contrast to CR 39 the quality of MAKROFOL does not vary so much from one batch to another. MAKROFOL is produced as an industrial foil in big amounts. At this time it is not yet possible to produce CR 39 in big amounts with constant quality. From one detector to another changes in thickness of a factor of 2 and more have been observed. In Table 2.1 the most important characteristics and in Table 2.2 the applied etching conditions of these three detector materials for radon measurements are presented.

2.2 Processing of the MAKROFOL track etch detectors

2.2.1 Electrochemical etching

A heavy ionizing particle creates along its pathway in a nonconducting material a tiny track of damaged material. The diameter of these tracks is in the order of 5 to 10 nm (F1 69). These damages react faster than other non damaged parts of the materials with certain solutions. This is used to enlarge the tracks as conical or cylindrical holes up to 1 to 30 μm ('conventional etching').

By applying an electrical field during the etching process it is possible to enlarge the tracks so much, that they can be seen by eye (To 70) ('electro-

	DETECTOR TYPE ¹⁾			
	LR 115 conv.	conv. CR 39.	ECE	MAKROFOL ECE
BACKGROUND N_0				
tracks/cm ²	20	309	58.7	12.9
1 S_0 -value	13.8	133	48.8	4.9
1 s_0 -value (%)	69	43	83	38
RADON SENSITIVITY ϵ_{Rn} ³⁾				
$\frac{\text{tracks} \cdot \text{cm}^{-2}}{\text{pCi} \cdot \text{l}^{-1} \cdot \text{d}}$	1.4	7.4	1.66	0.6
1 S_r -value	0.15	1.8	0.21	0.048
1 s_r -value (%)	11	24	12.6	8
α -SENSITIVITY ϵ_{\max} ²⁾				
tracks $\times 10^{-2}$	10.72	-	1.47	1.47
$\epsilon_{Rn}/\epsilon_{\max}$	0.16	-	-	0.41
DETECTED α -ENERGY RANGE E_α in MeV	1.5-3.8	0.1-10 ⁴⁾	0.5-3.4	0.5-2.8
LOWER DETECTION LIMIT ³⁾				
tracks/field size in cm ²	6/0.2	2/5-10 ⁻³	3/0.04	10/1
pCi·l ⁻¹ ·d	20	50	47.1	17

¹⁾ track etch detectors, LR 115 and CR 39 conventional etched, CR 39 and Makrofol pre-etched and electrochemical etched

²⁾ relative sensitivity at α -energies of 3 MeV (LR 115) and 2 MeV (CR 39 and Makrofol)

³⁾ for radon and daughters in the Karlsruhe diffusion chamber, foil position No 1, and a relative standard deviation of 50 %

⁴⁾ after Benton et.al., Int. Conf. of Solid State Nuclear Track Detector, Lyon, 1980

Table 2.1: Track etch detector characteristics for radon measurements in the KfK Diffusion Chamber.

DETECTOR TYPE	ETCHING TECHNIQUE		TRACK DIAM. μm	TRACK COUNTING FIELD cm^2	MAGNIFI- CATION
	CONVENTIONAL	ELECTROCHEMICAL			
LR 115	10 % NaOH 60°C, 2 hours	-	8	0.02	400x
CR 39	90 % 6N KOH 10 % C ₂ H ₅ OH 20°C, 3 hours	-	10	0.02	400x
CR 39	90 % 6N KOH 20°C, 30 min	10 % C ₂ H ₅ OH 20°C, 3 hours 600 V _{eff} , 5 kHz	50	0.5	40x
MAKROFOL	80 % 6N KOH 20°C, 1 hour	20 % C ₂ H ₅ OH 20°C, 3 hours	120	1.0	20x

Table 2.2: Description of applied etching conditions and track counting.

chemical etching'). This is a big advantage if a limited number of tracks has to be counted in a bigger area. The disadvantage of electrochemical etching is in contrast to conventional etching a track saturation at a density of about 3,000 tracks per cm^2 .

Electrochemical etching is mostly used for alpha particles and neutron induced recoils. For radon measurements in houses and in outside air track densities of hundreds per cm^2 are expected. Therefore the electrochemical etching procedure is applied.

The electrochemical etching process is influenced by many parameters, such as electrical field, frequency, solutions, temperature, detector material, etching time and so on. There is a good general view on these influences given by Tommassino in literature (To 81).

2.2.2 Etching system for processing large series of detectors

The system used for electrochemical etching consists of two parts, the high voltage generator for up to 2,000 V and up to 10 kHz and the etching cells. There are several designs of etching cells described in the literature (To 81). These have been designed for simultaneous etching of only very few detectors. Therefore these etching cells are not very convenient for large series.

A modular system of etching cells has been developed for processing large series of detectors (Fig. 2.4) (Ur 84a). It consists of two parts, the etching cell and the frame. Between every two plates (Fig. 2.5) and two rubbers, two detectors are pressed. The etching cell consists of a sandwich of 11 plates containing 20 detectors and is pressed between two steel plates (Fig. 2.6). For etching the cell is put into the frame. The electrodes of the cell are connected by springs through fuses to the generator. The fuses make sure that a short circuit in one part of the cell will not affect the rest of it. They switch off the electrodes. Etched through tracks or leakage in the cell can create such short circuits. The observed rate of short circuits in processing more than 20,000 detectors is below 1%.

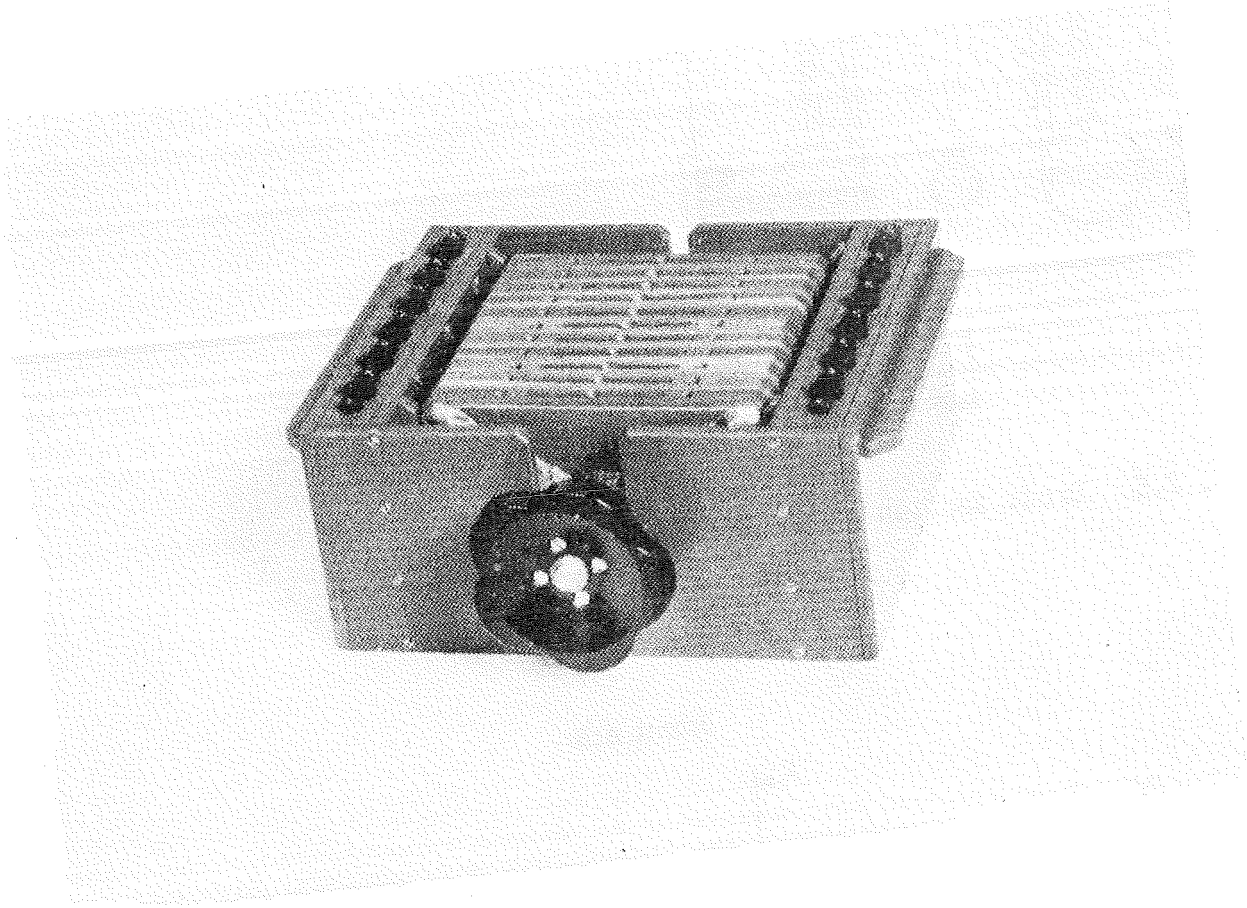


Fig. 2.4: Etching cell developed at KfK.

Schnitt C-D

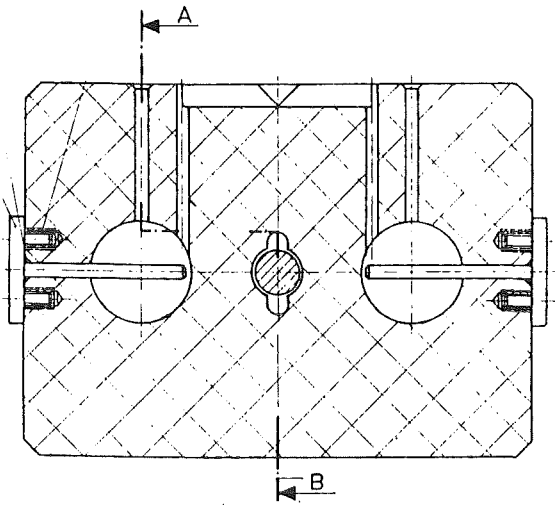


Fig. 2.5: Cross section of one etching plate.

Schnitt A-B

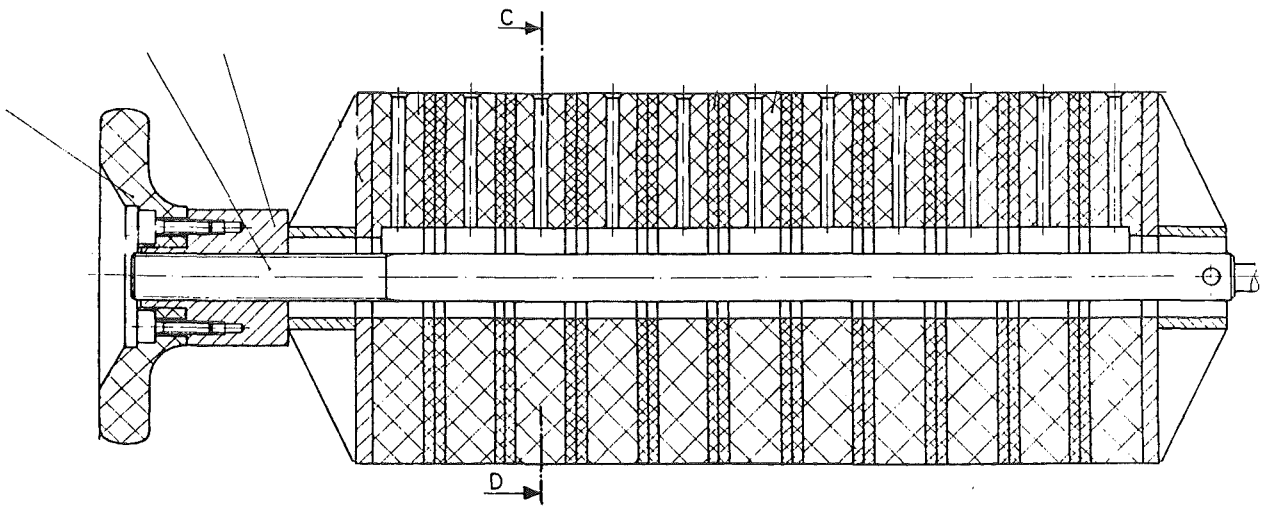


Fig. 2.6: Cross section of the sandwich.

The material used for the etching cell is PVC. The rubbers are made of soft PVC, the electrodes of stainless steel. During the etching the voltage, the current and the frequency are plotted for control purposes.

2.2.3 Counting of tracks

There is the possibility to count electrochemically etched alpha tracks using an automatic device. The main disadvantage of such a device is the high price. Therefore it is more suitable to count the tracks manually.

Using a microfiche reader/printer copies of the detectors were done at a magnification of 20 (Fig. 2.7). On this copy a field of 1 cm^2 is marked and counted by hand.

Radon daughters plated out on the surface of the diffusion chamber result in alpha particles entering the detector foil under relatively flat angles of incidence. The orientation of the alpha source to the detector results in a selected detection of alpha particles with respect to alpha energy, and a critical angle of incidence. The number of alpha particle tracks found in the detector foil shows, therefore, a maximum in the centre of the foil, decreasing with increasing distance from the centre. This effect was investigated by counting the track density along the field diameter over small areas of 8 mm^2 (Fig. 2.8). It can be seen from the track distribution in Fig. 2.8 that the track maximum is found in the centre of the detector. Consequently, any change in the detector position inside the diffusion chamber and/or in the field selected for the track counting may result in counting errors outside the range of the estimation of the standard deviation. By counting the tracks in concentric areas the relative track density decreases from 110% for a field of 0.25 cm^2 , to 100% for 1 cm^2 and 90% for 3 cm^2 .

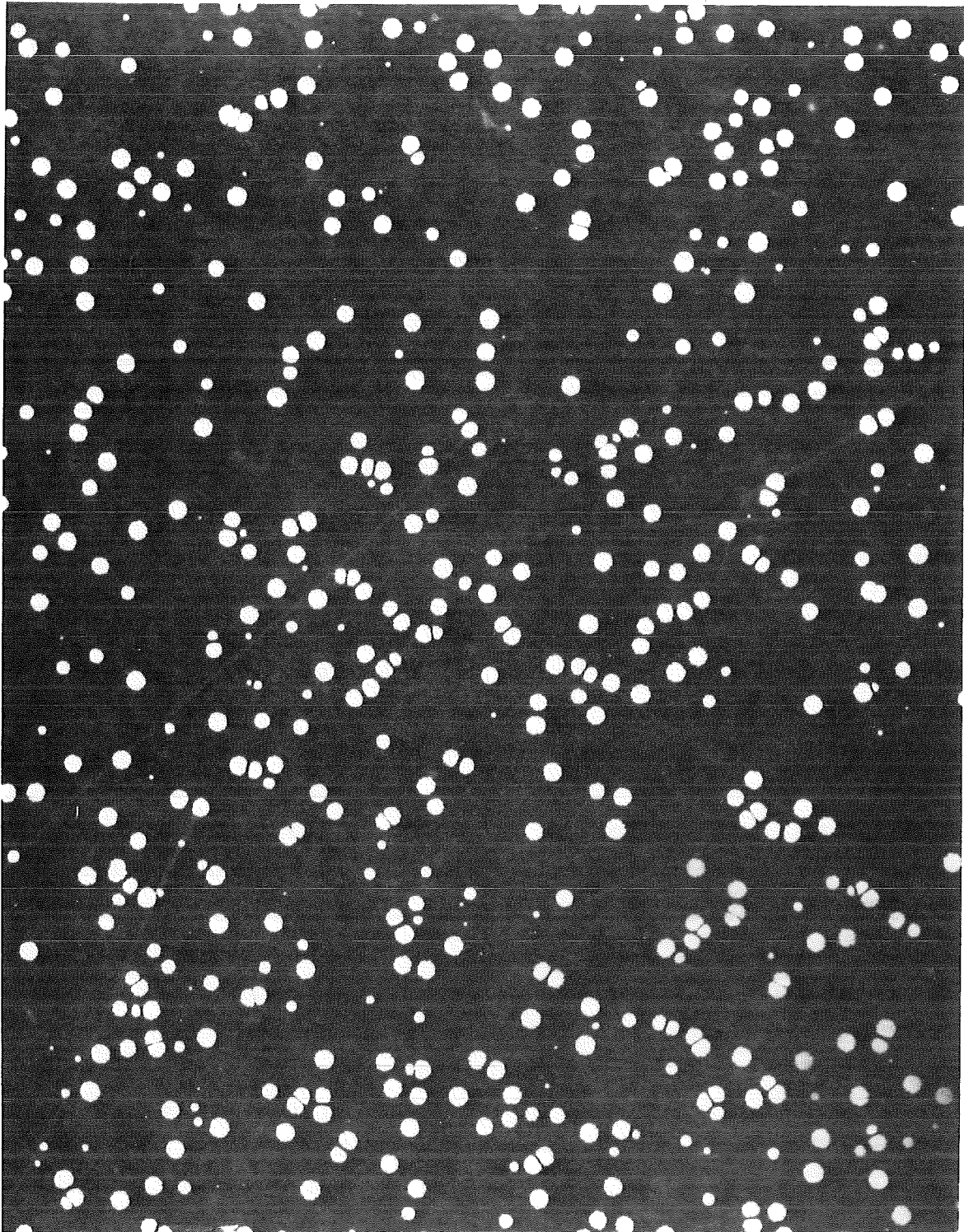


Fig. 2.7: Part of a microfiche reader/printer copy with alpha tracks at a magnification of 20.

2.3 Calculation of the mean radon concentration

2.3.1 Radon exposure

The measured quantity of the radon dosimeter is the time integral of the actual radon concentration, called exposure. The radon exposure X is given by:

$$X_{\text{Rn}} = \int_0^T C(t) dt \quad (2.1)$$

where X = radon exposure in $\text{Bq/m}^3 \text{ d}$,
 $C(t)$ = radon concentration at the time t ,
 T = irradiation time.

Assuming linearity between radon exposure and the number of tracks counted the sensitivity ϵ of the diffusion chamber is given by:

$$\epsilon = X_{\text{Rn}}^{-1} \left(\frac{N_1}{A_1} - \frac{N_0}{A_0} \right) \quad (2.2)$$

where ϵ = radon sensitivity in $(\text{tracks/cm}^2)/(\text{kBqm}^{-3} \text{ d})$,
 N, N_0 = number of tracks counted in the field A , background tracks in the field A_0 , respectively,
 A, A_0 = area counted in cm^2 for the total number of tracks and background tracks, respectively.

The results of calibrations at BGA Neuherberg, EML New York USA, NRPB Didcot England and KfK are presented in Fig. 2.9 as a function of radon exposure. On the basis of the experimental results the sensitivity of the alpha particle detector in the diffusion chamber was calculated using a "Weighted Least Squares" curve fit and found to be

$$\epsilon = 16.2 \frac{\text{tracks/cm}^2}{\text{kBqm}^{-3} \text{ d}}$$

with a computed 3 sigma value of +5%.

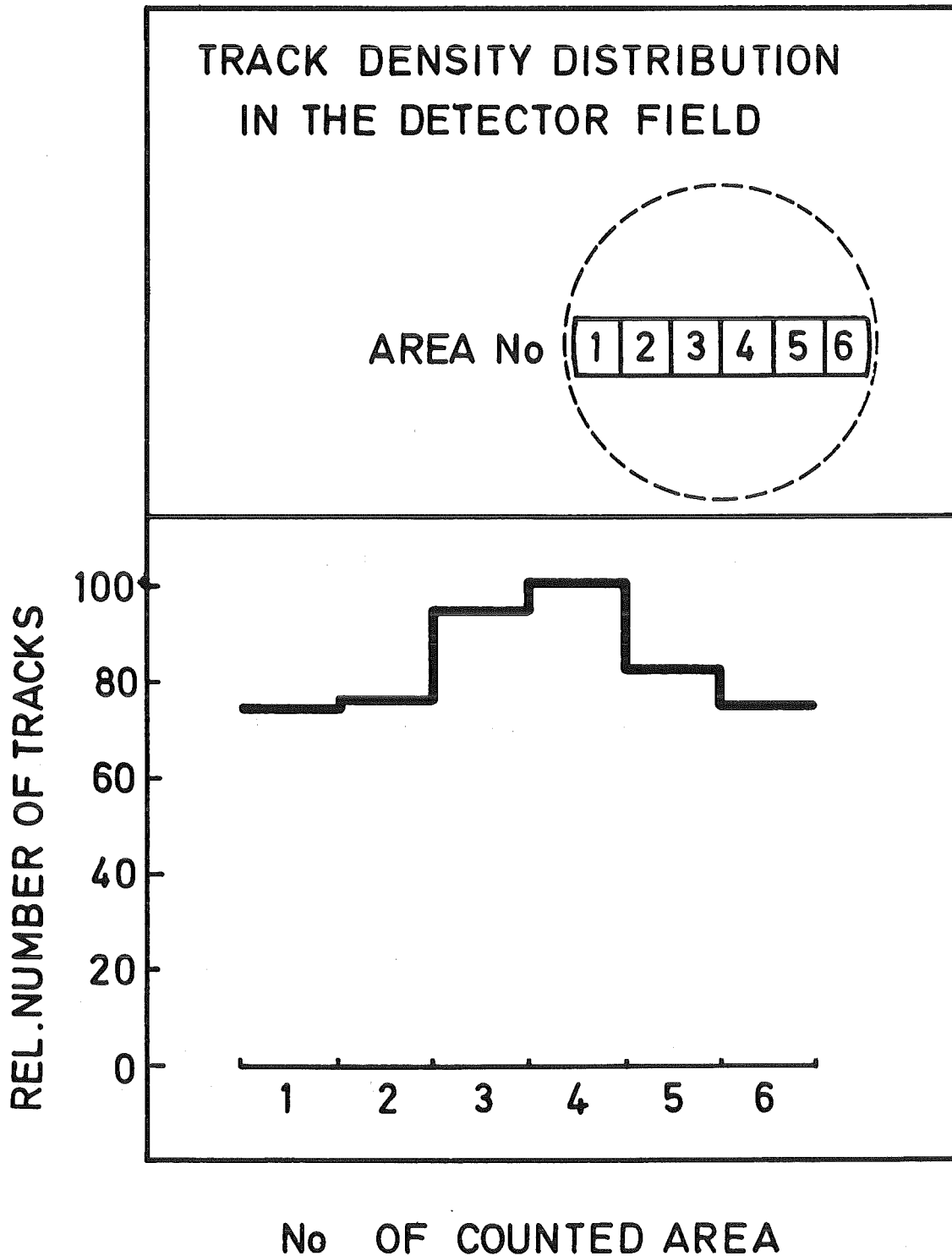


Fig. 2.8: Inhomogeneity of the alpha track density counted in partial fields of 8 mm^2 along the field diameter.

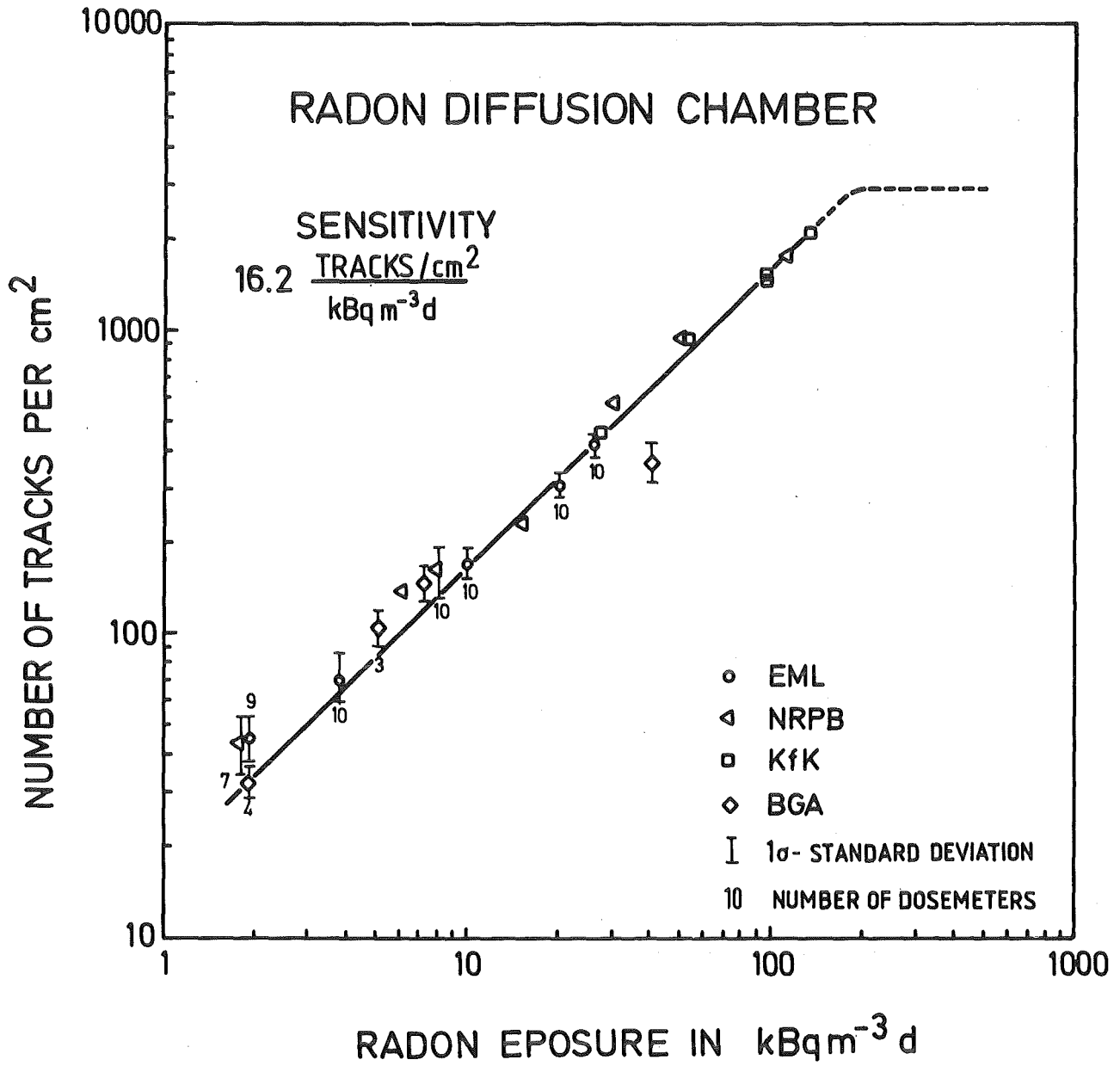


Fig. 2.9: Calibration of the KfK Diffusion Chamber.

2.3.2 Uncertainty of the radon measurements

The total measuring uncertainty of the track counting was investigated experimentally by measuring two sets each of ten detectors. One set is unirradiated and the other is irradiated under identical conditions. Taking into account the statistic uncertainty of track counting for the total tracks ($N + N_0$) the relative measuring uncertainty is given for low track numbers by the standard deviation of the background reading S_0 and for the high track numbers by the relative standard deviation s of the irradiated set:

$$s(N) = \frac{100}{N} (N + N_0 + S_0^2 + s_i^2 \times N^2)^{1/2} \quad (2.3)$$

where N , N_0 = number of radiation induced or background tracks,

S_0 = standard deviation of the background reading N_0 ,

s_i = relative standard deviation caused by systematic uncertainties.

The tracks of both detector sets have been counted in the same field size. The relative standard deviation $s(N)$ vs. number of tracks can be calculated on the basis of the formula and the experimental values S_0 and s_r of the unirradiated and irradiated set. The relative standard deviation s_i is given by the s_r value of the irradiated set with the track number N_r :

$$s_r^2 = s_i^2 + N_r^{-1} \quad (2.4)$$

s_i is the total systematic uncertainty resulting mainly from the scatter of the individual detector sensitivity within the set as well as from the etching and counting technique. The $s(N)$ -curve can be used to estimate the lowest detectable track number N_L for a relative standard deviation of 50% (1 s value). With the radon sensitivity of the track detector in the diffusion chamber the lowest detectable radon exposure X_L is then given by:

$$X_L = N_L \times \epsilon_{Rn}^{-1} \quad (2.5)$$

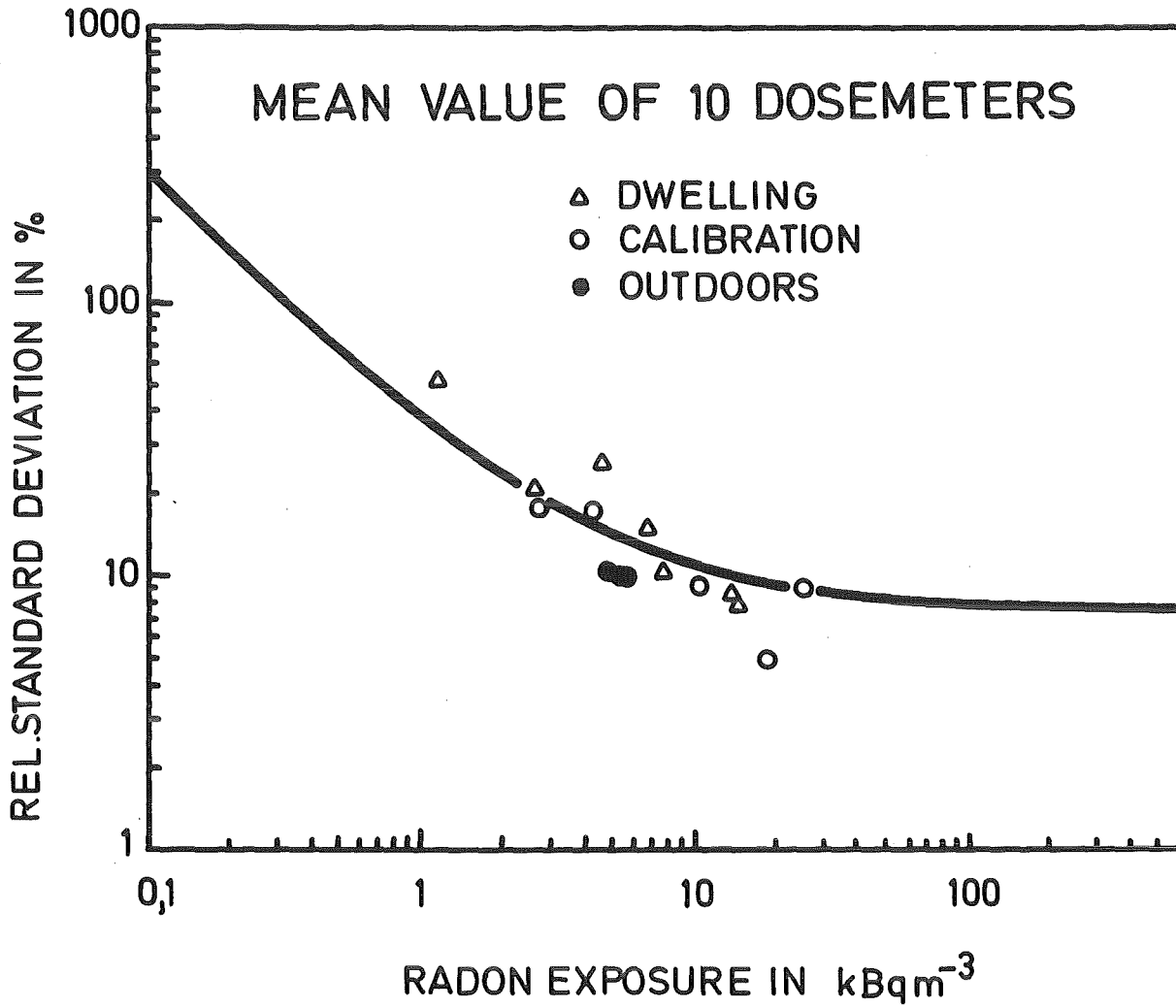


Fig. 2.10: Calculated relative standard deviation of detectors from the KfK Radon Diffusion Chamber as a function of radon exposure, comparison of measured standard deviations of ten dosimeters with estimated values.

In Fig. 2.10 the relative standard deviation is presented as a function of the radon exposure. The s-values in the lower exposure range depend mainly on the subtraction of the background tracks and the corresponding counting statistic which can be improved by counting more tracks in several fields. The constant s-values at higher exposures are caused by systematic errors.

Another uncertainty of the radon measurement is the sensitivity of the dosimeter to thoron. It is expected that the sensitivity to thoron is only about 10% of the sensitivity of radon. Tracks resulting from thoron are regarded as radon tracks.

2.4 Reproducibility

Reproducibility tests have been performed for different exposure conditions such as indoor, outdoor and calibration exposure. Every time ten dosimeters have been exposed together. The resulting standard deviations are presented together with theoretically expected uncertainty in Fig. 2.10.

As expected from counting statistics and from the scatter of the background track density reproducibility for low radon exposure is rather poor. For exposures in the order of 5 to 10 kBq/m³ it follows direct counting statistics. For high exposures there is a saturation effect. It no longer follows counting statistics. This effect is taken into account when the uncertainty of the measurement is calculated.

2.5 Fading of the track etch detectors

A significant latent fading of neutron induced recoil and alpha-particle tracks have been observed in the nuclear track emulsion as well as in most of the solid state track etch detectors. The loss in information in the period between irradiation and development depends significantly on ambient

temperature and humidity. Latent tracks in non-photographic track etch detectors are more stable against influences of temperature and air humidity. The temperature fading may vary, however, with the type of detector material, the kind of etching, namely conventional or electrochemical and with the counting technique, namely manual counting in a microscope, automatic scanning or spark counting. Conventionally etched MAKROFOL E recoil track detectors, for instance, have been found to be free of fading up to storage periods of three years at ambient room temperatures. Only low fading has been found for MAKROFOL E even at higher temperatures of 50 °C in contrast to conventionally etched cellulose acetate and to the NTA film (Sa 74).

The latent fading has been investigated within a 40 days period at ambient temperatures of 5 °C, 20 °C, 35 °C and 50 °C and relative humidities of 0%, 50%, and 95% (Ur 83). The detectors have been irradiated with Cf-252 neutrons for the registration of neutron induced recoils and with alpha particles from Am-241 with respect to an application of (n, alpha) radiators in neutron dosimetry as well as to the large scale use of MAKROFOL as detector in the KfK Passive Radon Diffusion Chamber. The irradiations have been performed at different times and at the end of the storage periods all detectors have been etched simultaneously at least for each storage condition.

The fading results are presented here as the ratio of actual track density and reference track density found immediately after irradiations. The marks indicate the scatter of three detectors, and the dashed lines the uncertainty in estimating the number of reference tracks. Taking into account the random statistical uncertainty of track counting and the systematical errors expected from influences of foil quality, etching conditions and track counting, no significant fading can be observed in the temperature range between 5 °C and 50 °C. The latent fading has been found to be within the measuring uncertainty. The humidity dependence of the latent fading of alpha particle tracks is shown in Fig. 2.11. The scatter of the reference detectors is +7%. The figures for the other conditions are similar. In conclusion, no significant fading has been found for electrochemically etched MAKROFOL E up to temperatures of 50 °C and relative humidities of 95%.

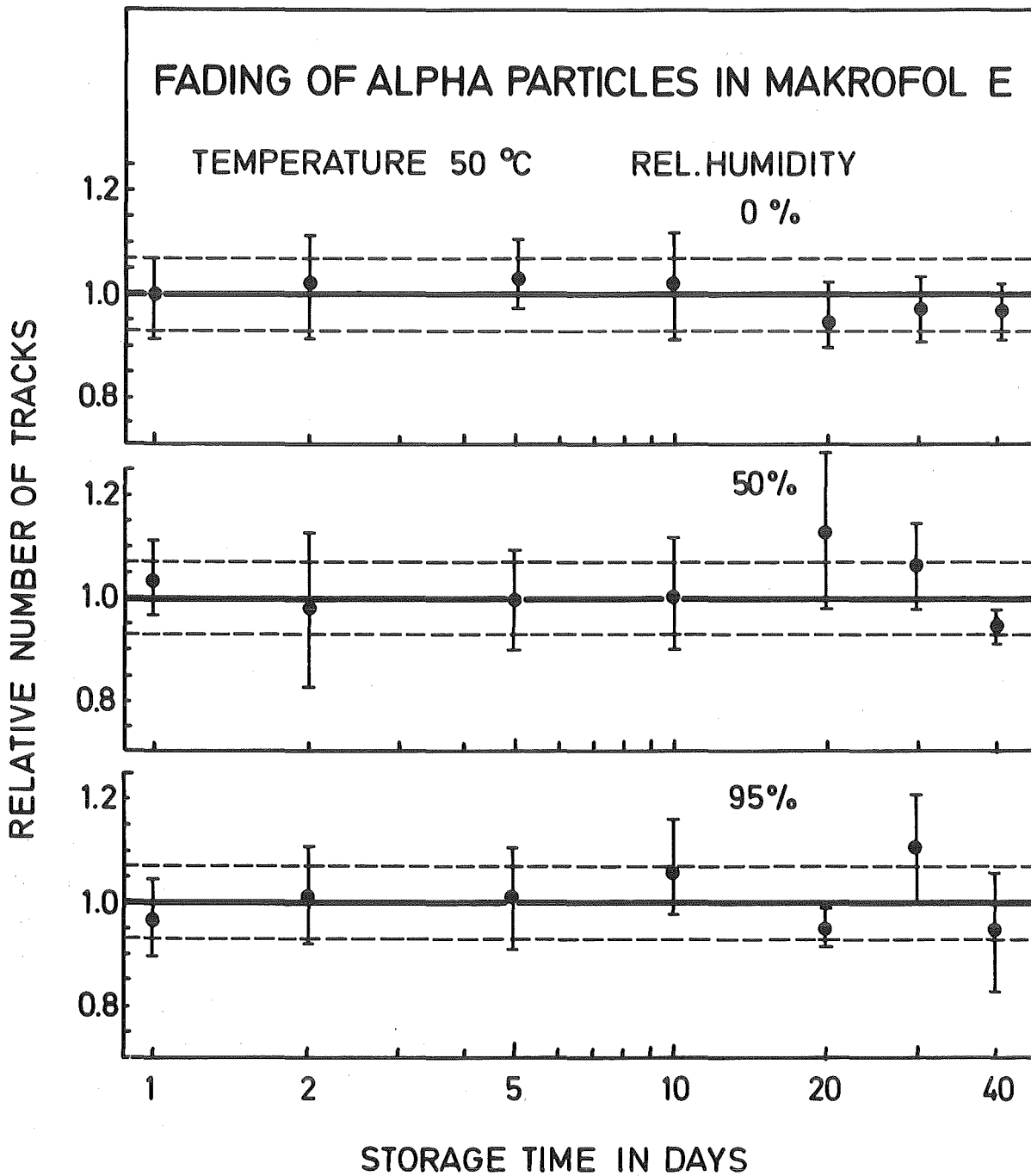


Fig. 2.11: Latent fading of alpha particle tracks in electrochemically etched MAKROFOL E for different humidities at a temperature of 50 °C.

3. MEASUREMENTS IN MINES

3.1 Brazilian mines

Radon concentration measurements were performed in an open pit mine and milling complex using diffusion chambers developed by KfK. Measurements included areas both indoors and outdoors covering the entire operations from the ore sampling before the mineral extraction up to the chemical and physical separation of uranium for the yellow cake fabrication, and also around the dam constructed for the lake used for sedimentation of the radium extracted during the separation process.

The results of twelve months survey are shown in Table 3.1. The two main seasons of the region were considered: Rainy season (January to June) and Dry Season (July to December).

As can be expected the radon concentration is higher during the dry season, and elevated levels are found in the ore storage bins and especially in the crushing and milling circuits.

3.2 Monitoring in German mines and mining areas

3.2.1 Environmental monitoring

Since 1979 the environment of several German exploration mines was controlled for radon using the KfK Passive Diffusion Chamber for more than two years each (Ur 84b). In Fig. 3.1 the temporal variations of the mean radon concentration at the fence of the mining area and in a distance of up to 300 m from it are plotted. The mine is situated in a flat rural country site. Each plotted concentration is a mean value of 20 single measurements.

The two curves are nearly parallel. From the difference of both the source strength of the mine as a radon emitter for the environment can be estimated. The decrease of the radon concentration in 1983 was not due to the closing of the mine in December 1982 as could be assumed. The reason for

Area	Radon concentration (Bq/m ³)			
	Rainy season	2 σ	Dry season	2 σ
<u>SAMPLING PROCESS</u>				
Infrared drying	159	12	180	16
Dry crushing	176	14	189	17
Pellet fabrication for X-ray	225	16	283	20
Storage room	209	16	239	19
<u>MINING AREA</u>				
Post 1	103	8	165	12
Post 2	112	8	152	11
Post 3	96	7	282	21
Ore sample storage	205	17	311	25
<u>FIRST CRUSHING</u>				
Operator's cabin	589	40	773	63
Basement	257	20	399	32
Stacker's cabin	78	5	153	11
<u>SECOND CRUSHING</u>				
Operator's cabin	145	11	174	14
<u>MILLING (HUMID)</u>				
Milling discharge	260	19	311	25
<u>CHEMICAL PROCESS</u>				
Homogenizer A	90	6	68	4
Homogenizer B	58	4	50	4
H ₂ SO ₄ process (A+B)	69	4	63	4
H ₂ SO ₄ process (C+B)	74	5	74	5
<u>PHYSICAL SEPARATION</u>				
Band filter (A+B)	67	5	80	5
Band filter (C+D)	61	5	94	7
<u>RADIUM SEDIMENTATION DAM</u>				
Post 1	99	8	114	8
Post 2	130	10	193	15
Post 3	138	10	213	16
Post 4	72	5	102	8
<u>TRANSPORT DIVISION</u>				
Supervisor's office	80	6	535 (closed)	40
Garage	51	5	59	4
Control room	234	17	314	25
Dining room	101	8	128	9
Maintenance area	75	5	108	8

Table 3.1: Open pit and milling complex.

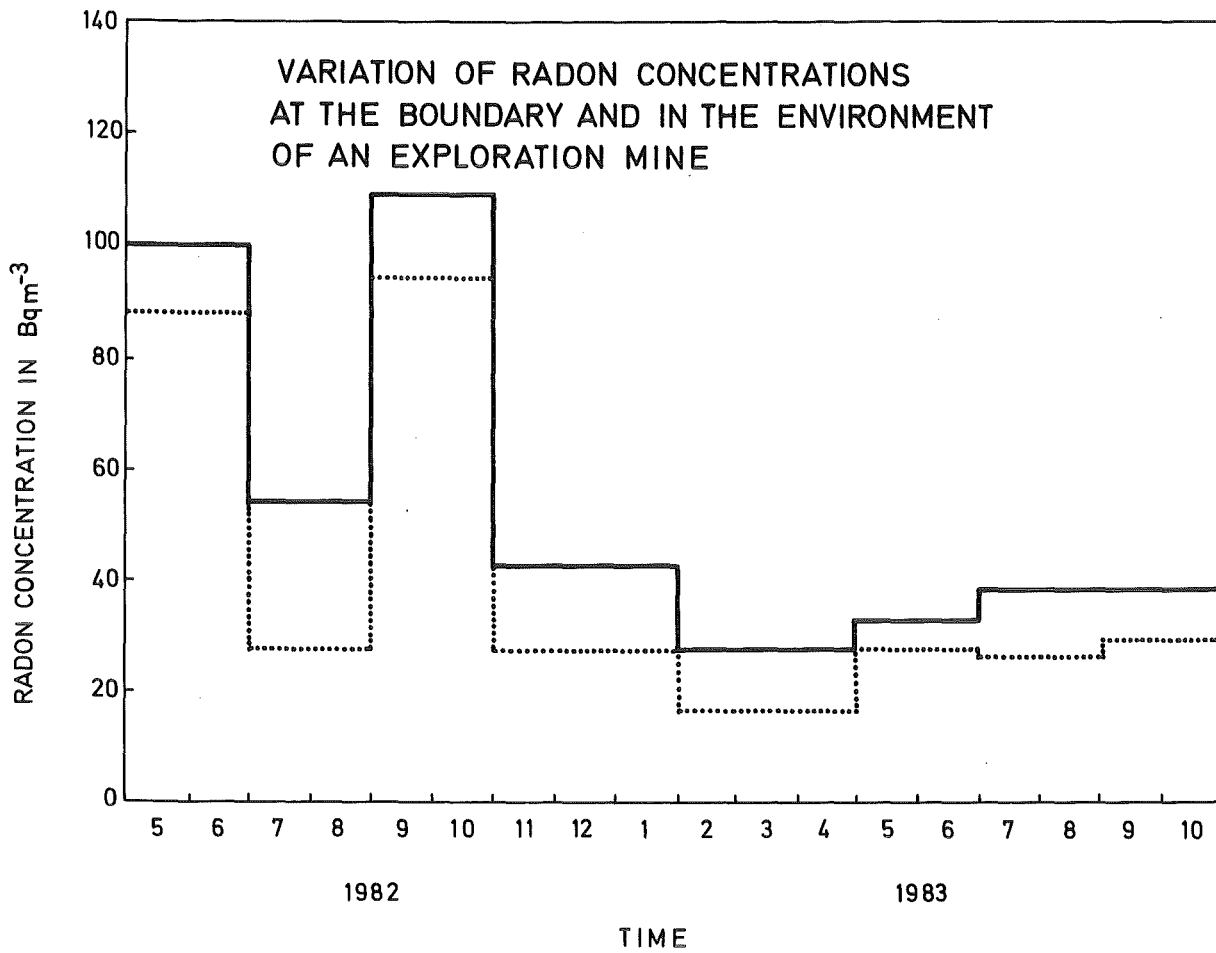


Fig. 3.1: Seasonal variations of the mean radon concentration at the fence of a mining area and in a distance up to 300 m from it, flat country side.

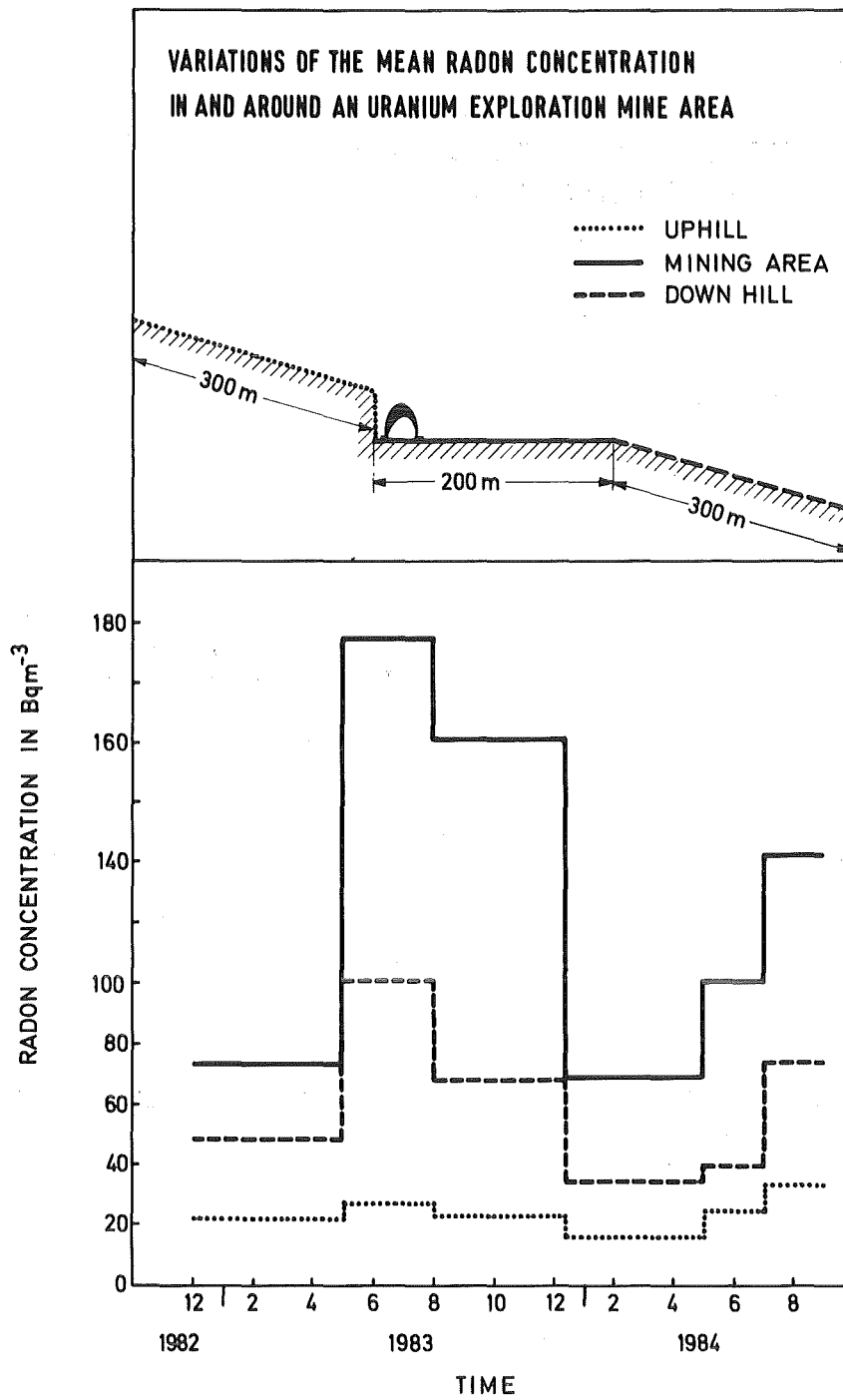


Fig. 3.2: Seasonal variation of the mean radon concentration in and around a uranium exploration mine, mountain valley.

the decrease were very different weather conditions in 1982 and 1983 especially wind and rain. Also other data from radon measurements in outside air integrated over periods up to one year indicate a strong dependence on meteorological parameters as amount of rain, number of days with rain and calm.

In Fig. 3.2 the temporal variations of the mean radon concentration in and around a uranium mining area in contrast to the previous one in a mountain valley are presented. The radon concentrations are strongly affected by wind, as the main wind direction is downhill. The downhill concentrations are apparently affected by the mine. Within the mine boundaries there is a dump of cut off ore. The exhalation of radon from this dump is influenced by seasonal weather conditions. In winter it is covered by snow. The exhalation is then very poor compared to summer data, so the winter values can be dedicated to the rather constant emission of the mine.

3.2.2 Monitoring in mines

While excavating side stopes into ore body of a ramp like uranium exploration mine, in addition to the official Instant Working Level Meter (IWLM) measurements radon monitoring with passive dosimeters were performed in monthly time intervals. Fig. 3.3 shows the monitoring scheme and the measuring positions at the ramp and outside with results from August 1982. Having a radon concentration of the entering ventilation air of 20 Bqm^{-3} a monthly mean output concentration of about $2,300 \text{ Bqm}^{-3}$ in an especially ventilated lower part of the ramp was achieved, while in the main part of the mine the concentration rose from 400 up to $1,500 \text{ Bqm}^{-3}$ at the mouth of the tunnel. On the mine site in open air the radon concentration is increased by mine ventilation by a factor of 6. The monthly integrating measurements assured the mining company that the ventilation technique was sufficient with respect to international dose limitations.

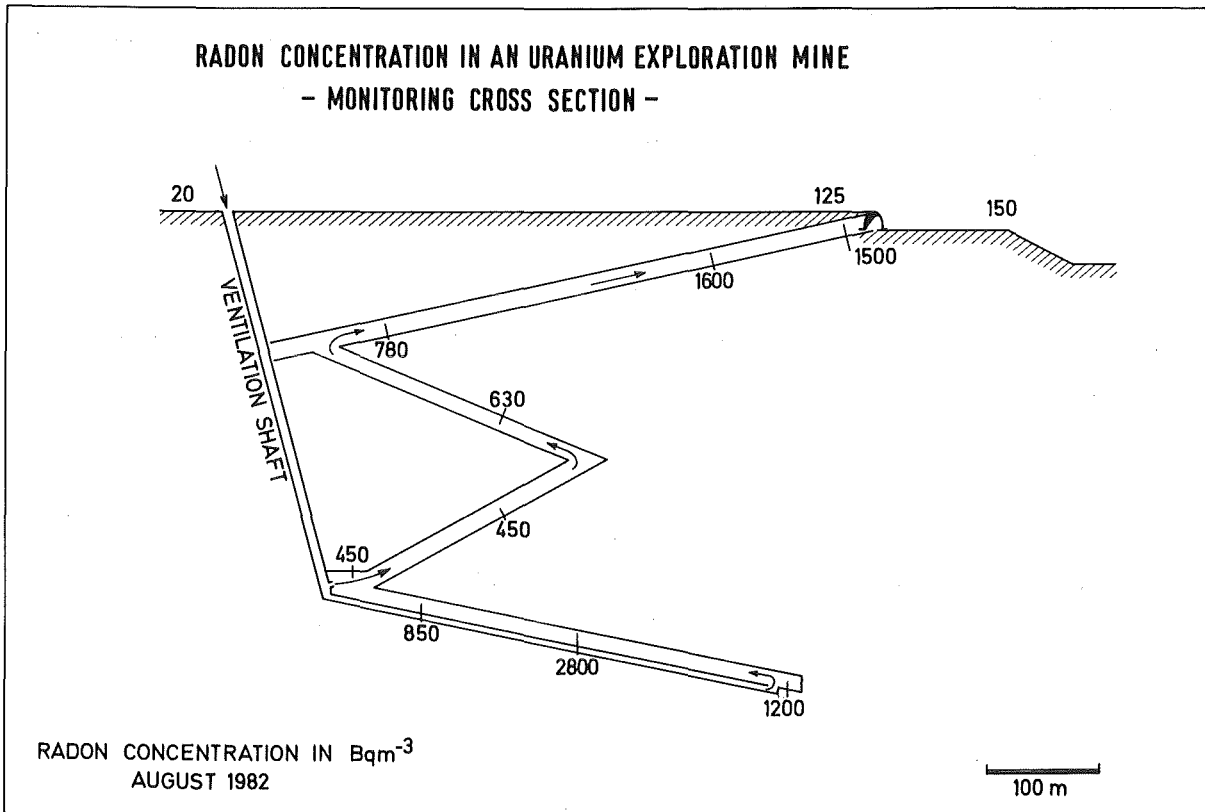


Fig. 3.3: Mean radon concentrations in a uranium exploration mine, August 1982.

The passive dosimeters were also tested as a short time i. e. daily monitor in a high exposed galery. It could be shown, that the radon concentrations deviated from the three times per shift performed IWLM measurements. These results were remarkably lower than the results from the dosimeters. While the results from the IWLM measurements varied from 0.3 to 24 WL within five days, the integrating dosimeters showed results from 66 to 420 kBqm⁻³. These results indicate, that from a few IWLM measurements in a mining area with probably strong variations in radon concentration may underestimate by far the lung exposure of the workers.

3.2.3 Personal dosimetry

The statistical evaluations of all surveillance data of a uranium exploration mine with strong variations in radon concentration from the years 1979 to 1983 resulted in an extreme doubt on the reliability of the measurements done using an Instant Working Level Meter to determine the exposure of individual miners to radon daughter products. There was for example no correlation found between output of ore and exposure. The monthly lung exposure of all miners, presented in Fig. 3.4, results in a logarithmic distribution. In consequence some of the miners were equipped with CEA personal radon dosimeters. In addition each working place was monitored twice a day using an Instant Working Level Meter (Fig. 3.5 and Fig. 3.6). There was no correlation found between these measurements and the CEA dosimeter (Fig. 3.7).

4. MEASUREMENTS IN HOUSES

4.1 Brazilian houses

For the Brazilian survey homes were chosen initially in three cities near the open pit uranium mine in the state of Minas Gerais, Poços de Caldas, Andradas, Caldas, and Rio de Janeiro. Each home was provided with three dosimeters: one placed in the living room, one in the bedroom and one in the

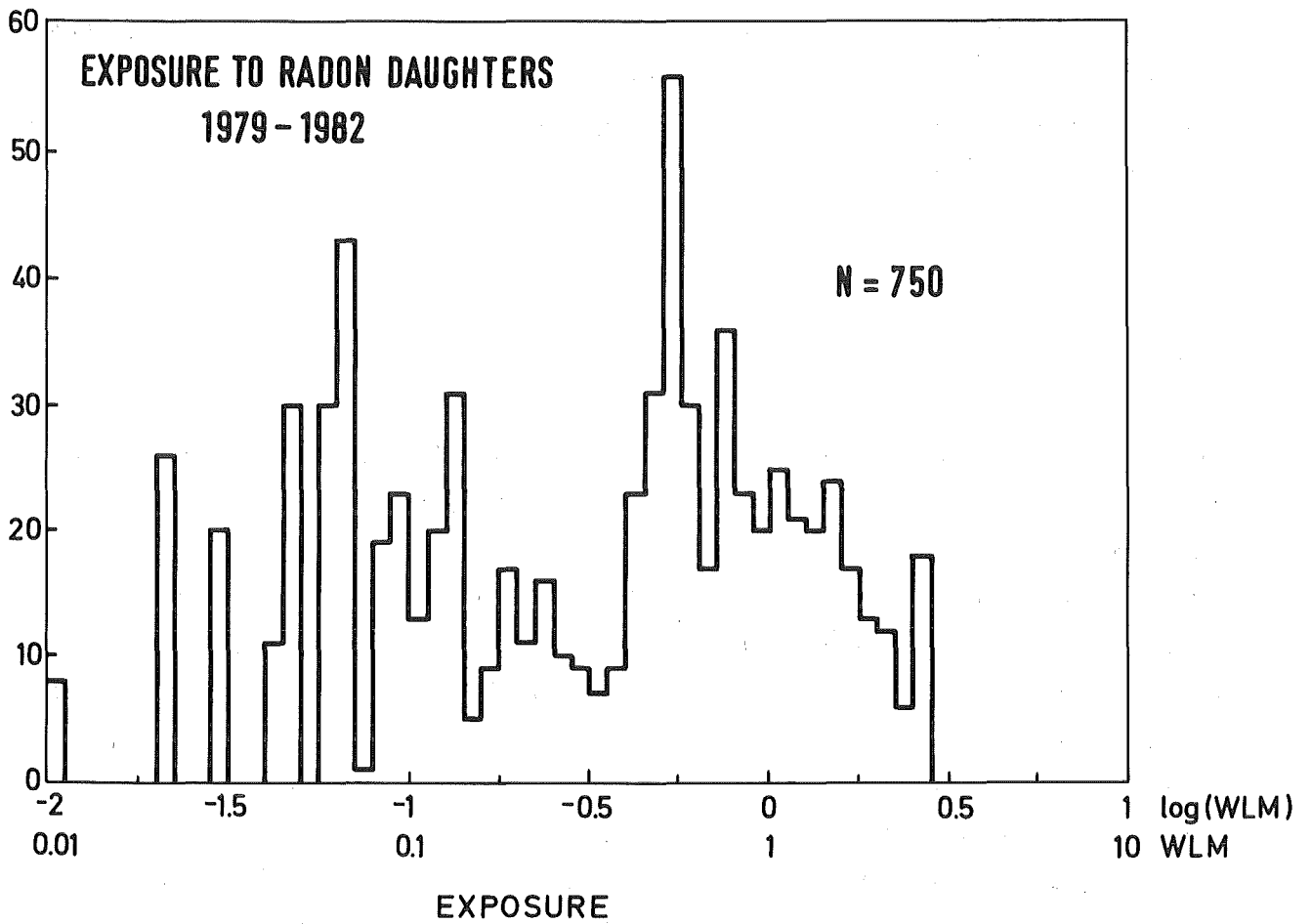


Fig. 3.4: Exposure of miners to radon daughters in 1979 to 1982.

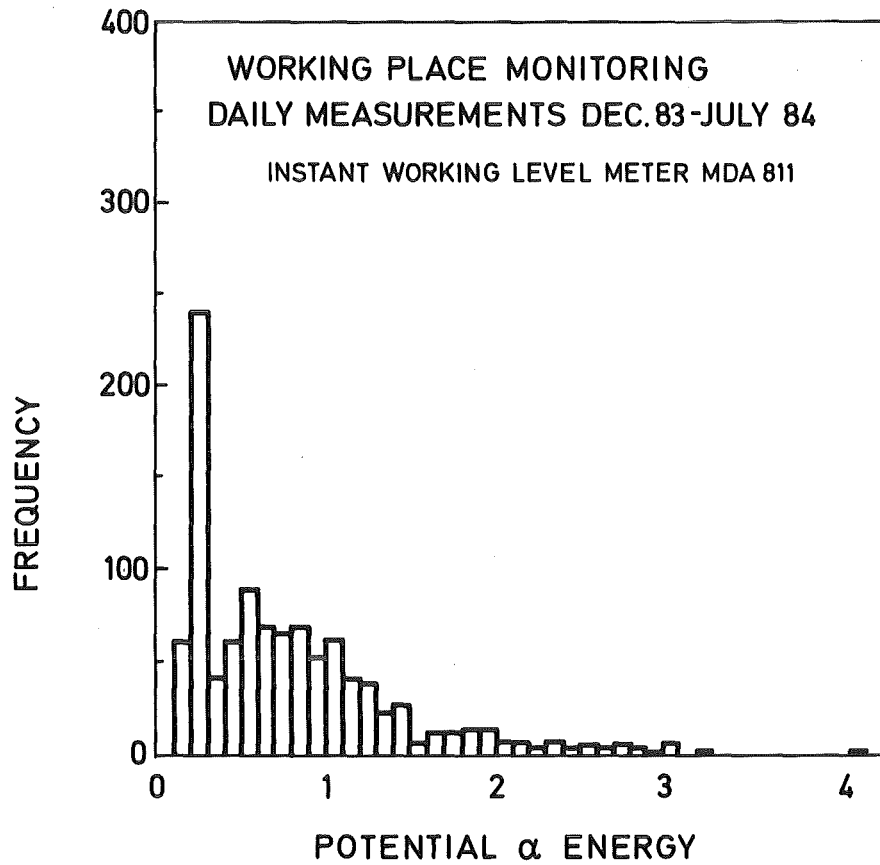


Fig. 3.5: Potential alpha energy from working place monitoring.

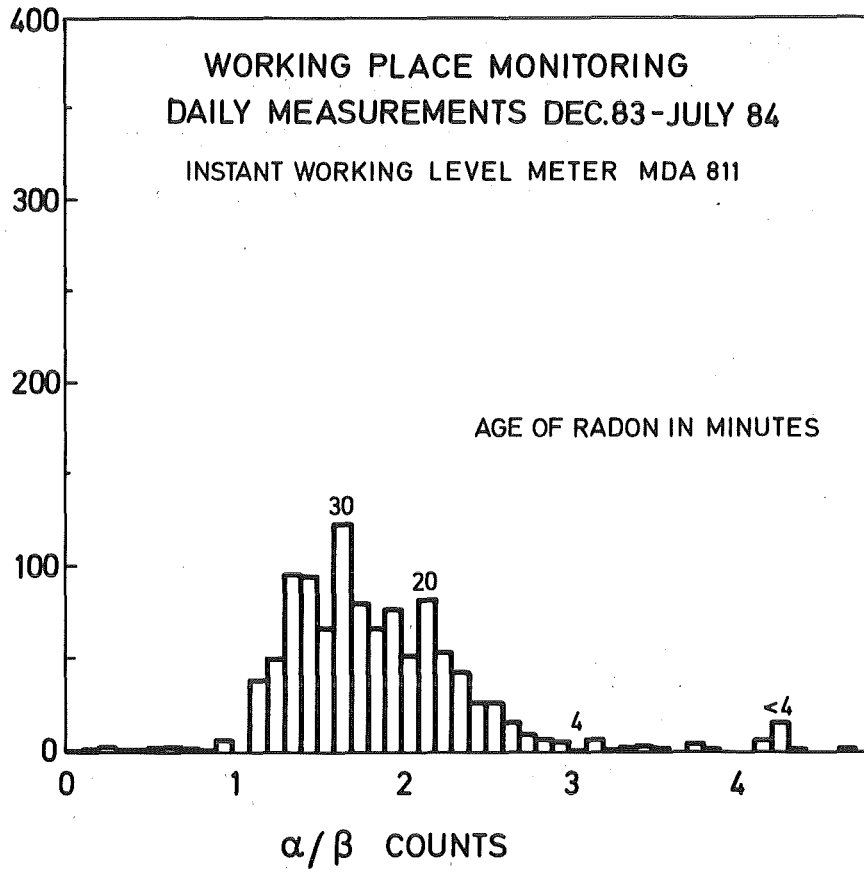


Fig. 3.6: Age of the air from alpha to beta counts.

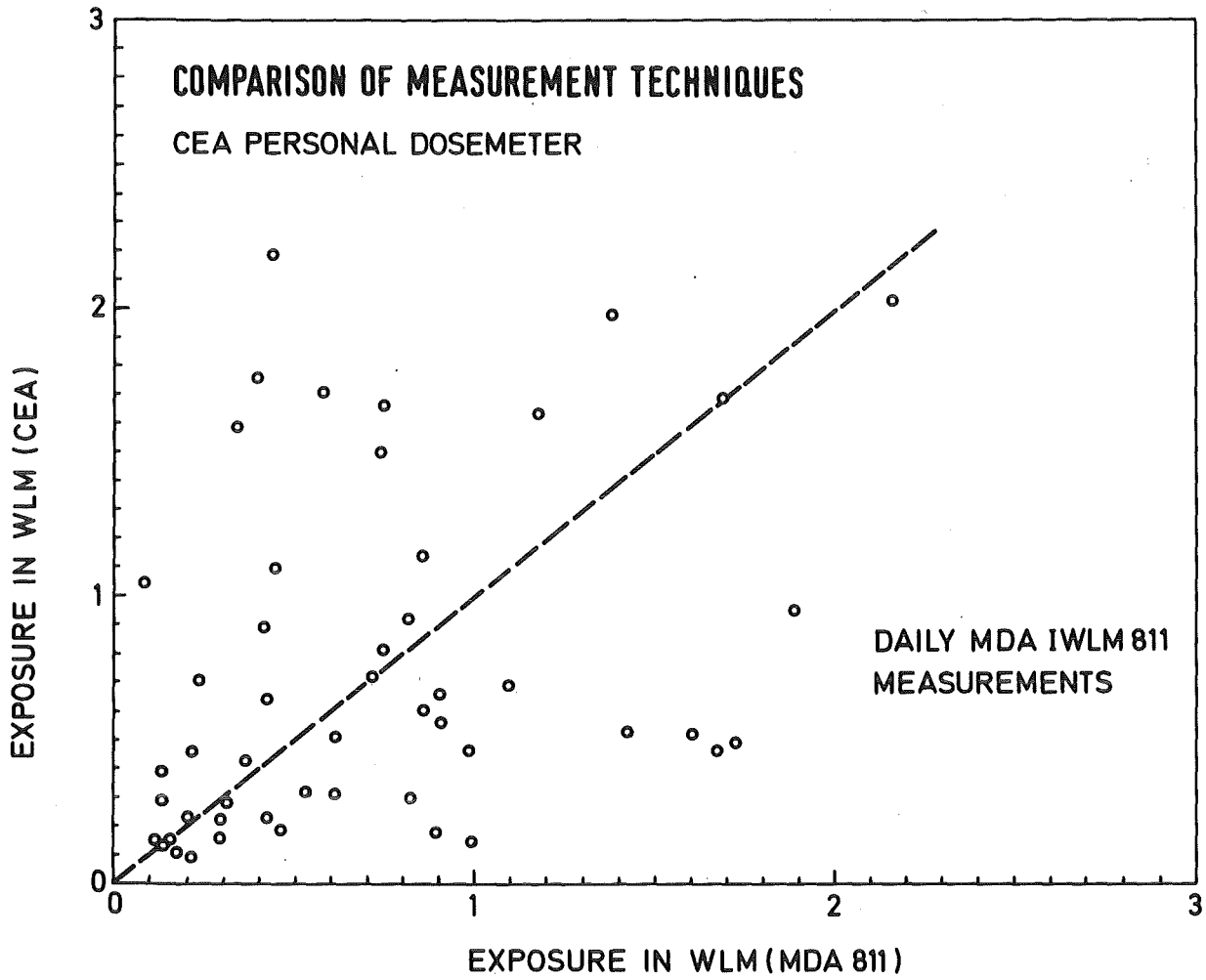


Fig. 3.7: Comparison of results estimating miner's exposure to radon daughters using the CEA personal radon dosimeter and MDA IWLM measurements.

bathroom. After four months the dosimeters were returned to the laboratory for processing. From the results of the measurements we can see that there is the pronounced variation of the radon concentration. In Rio de Janeiro, typical big town located on the seashore, low concentrations were found (24 Bq/m^3). In the cities in the vicinity of the uranium mine we have higher concentrations, being that in Poços de Caldas the mean radon concentration is 114 Bq/m^3 probably due to the fact that there is a geological fault containing a uranium vein passing under the city. Andradas (82 Bq/m^3) is a very small town located outside of the plateau where the mine is located, while Caldas (52 Bq/m^3) is also a small town located in the same plateau as the mine.

4.2 German houses

4.2.1 The German national survey

To organize the distribution and recollection of the radon dosimeters, nine laboratories in different parts of Germany are involved in the survey. In order to achieve an adequate distribution of the instruments, cooperation with the local administration of towns and countries turned out to be very effective. Different housing densities in various regions of Germany have been taken into account.

For the general survey each selected home was provided with two dosimeters, one of each was placed in the living room and one in the bedroom. After three months of exposure both dosimeters were returned to the laboratory with a questionnaire.

Complete results have been obtained from 5,972 homes. The distribution of the radon levels are approximately log-normal with 90% of dwellings having radon concentrations of less than 80 Bq/m^3 (Fig. 4.1). The median value is close to 40 Bq/m^3 , the geometric standard deviation 1.8.

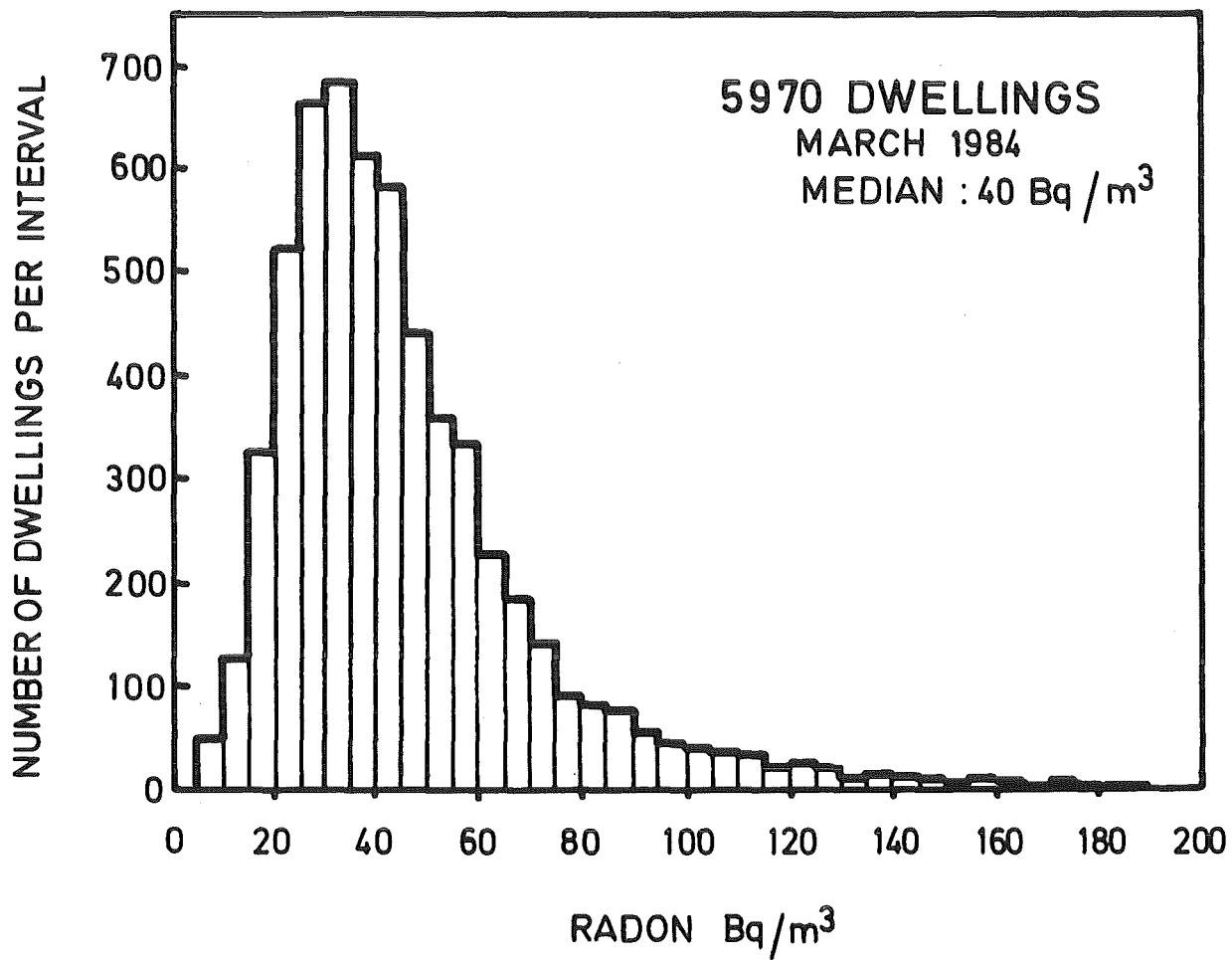


Fig. 4.1: Distribution of the radon concentration levels indoors.

According to Fig. 4.2 the calculated median radon concentration is significantly higher for detached houses (43 Bq/m^3) compared with multi-family houses (35 Bq/m^3) and high-rise buildings (33 Bq/m^3). The two main probable explanations for this observation are that detached houses have lower ventilation rates and are easier exposed to radon from the ground.

This fact is also reflected in Fig. 4.3. Highest radon concentrations are found in homes with direct ground contact. Apartments on upper floors show a decreasing radon level with increasing distance from the ground.

The importance of different types of foundations of a building is demonstrated in Fig. 4.4. The most frequent type of house built in Germany has a complete basement. Such a house has a median radon concentration of 38 Bq/m^3 , while houses without or partial basement show elevated levels, 43 Bq/m^3 and 50 Bq/m^3 , respectively.

The effect of different building materials on the radon concentration indoors is small. Corresponding to Table 4.1 high levels are only found in those houses built with natural stones and in wooden houses with loam (farmers' houses).

The regional variation of radon concentrations is not very pronounced. But there is an indication that lower levels are present in big towns, such as Hamburg, Munich or Berlin, in contrast to higher values found in rural areas. In addition we have found high radon levels in houses located in some isolated granite areas.

4.2.2 Radon concentration in outside air

Parallel to the measurements in homes extensive radon measurements in outside air have been performed. In a first step outdoor dosimeters have been distributed together with those for houses. Already after few exposures it could be seen from the data, that these measurements were not very re-

Material	Number of houses	Median (Bq/m ³)	Sigma (geom.)
Brick	2,229	40	1.8
Limestone	786	37	1.7
Pumice Stone	960	47	1.7
Slag Brick	54	37	1.8
Concrete	349	38	1.8
Areated Concrete	276	40	1.8
Loam (+ Wood)	43	57	1.8
Wood	150	29	1.8
Natural Stone	95	61	2.4
Gypsum	76	34	1.8

Table 4.1: Radon concentration in houses built from different construction material.

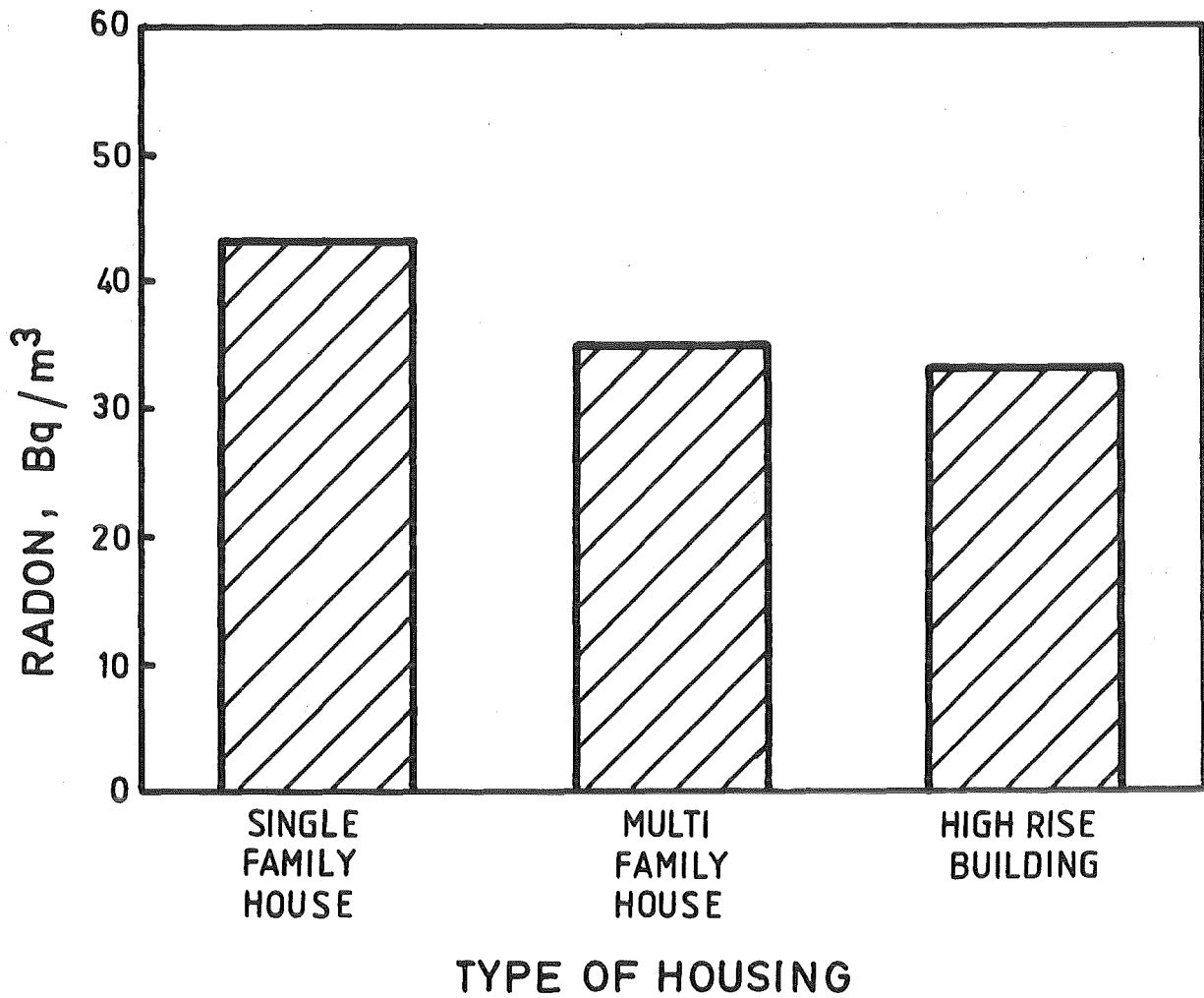


Fig. 4.2: Median radon concentration levels in different types of houses.

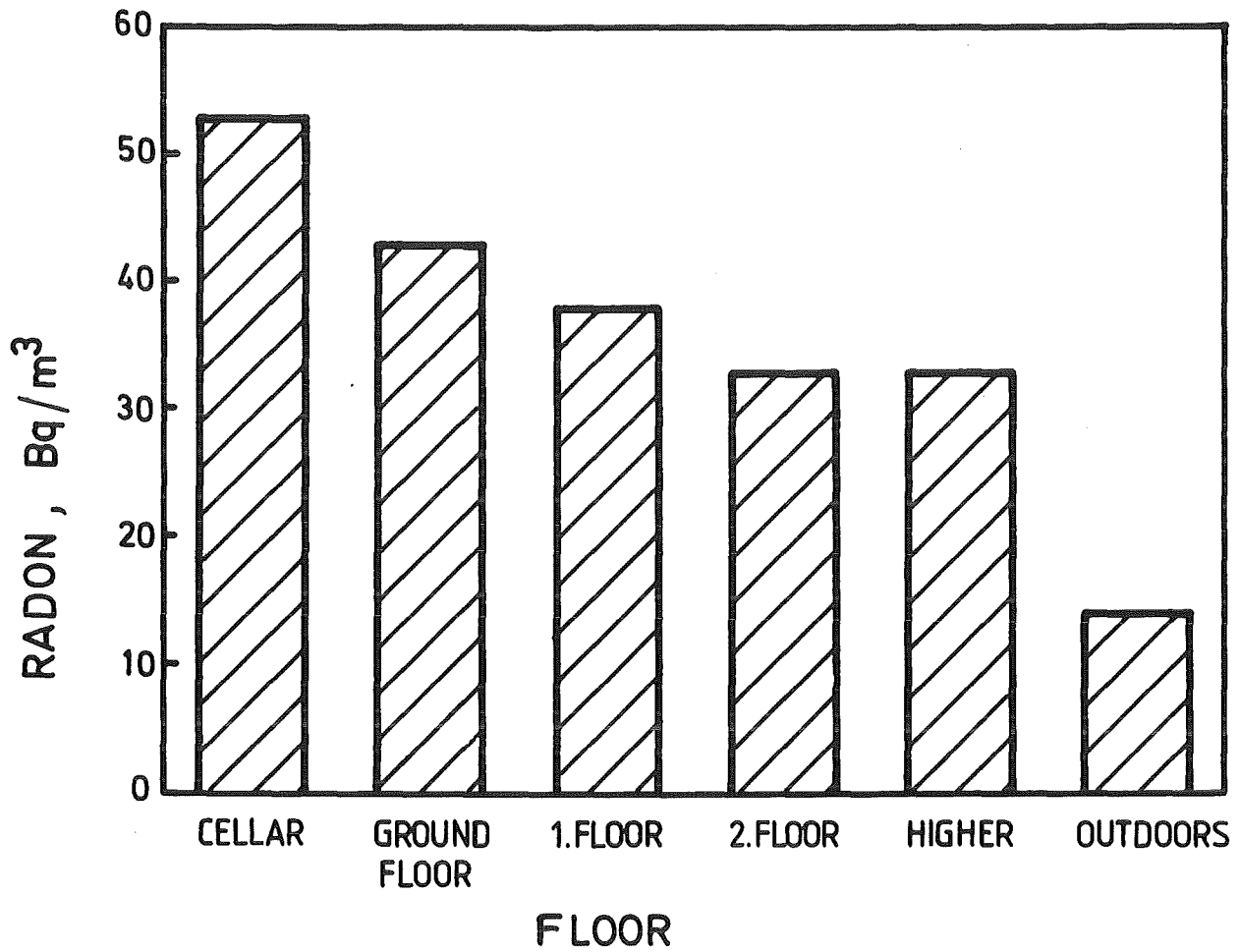


Fig. 4.3: Median radon concentration levels indoors depending on different distances from the ground.

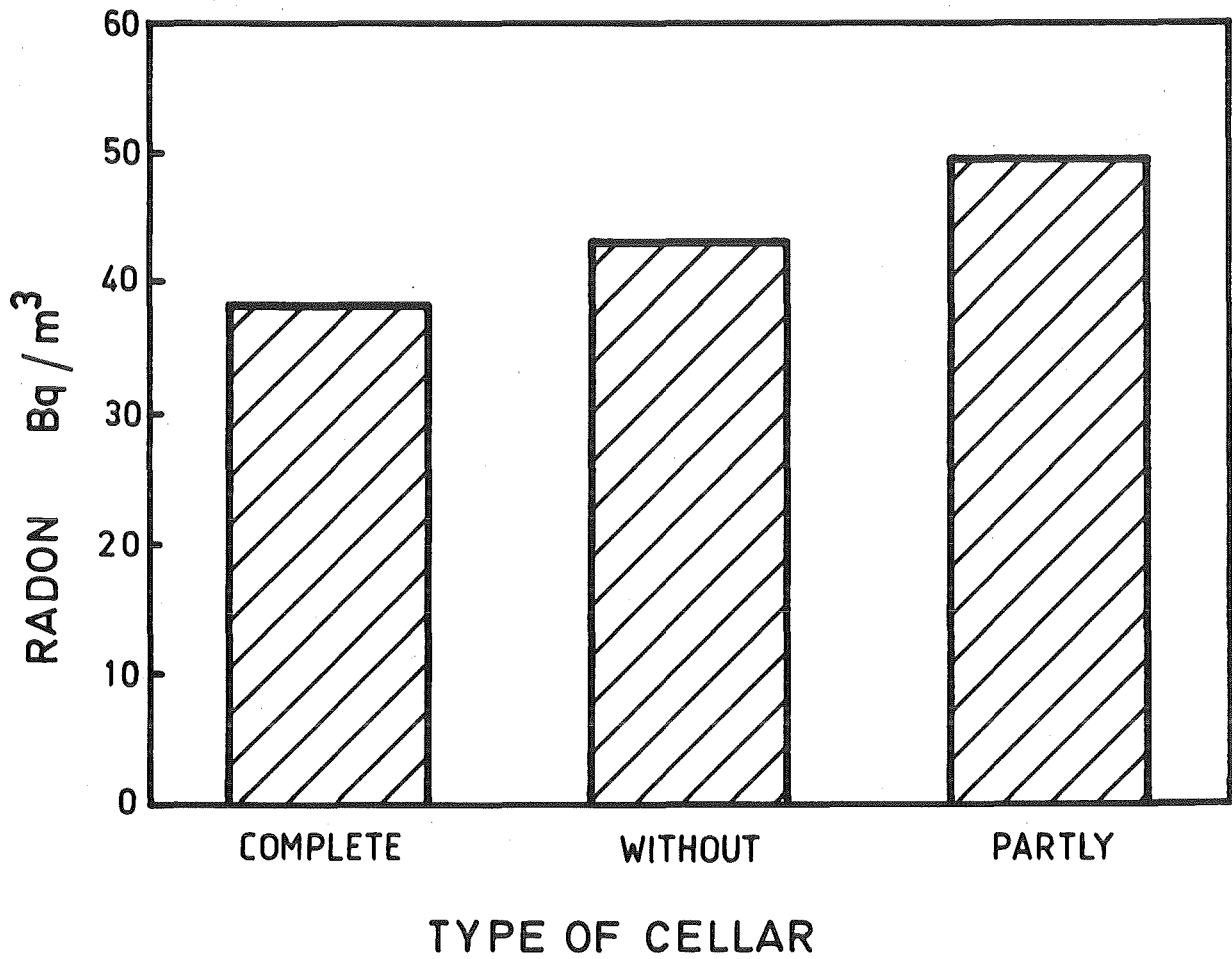


Fig. 4.4: Median radon concentrations in houses with different types of basement.

reliable. There are several reasons for this, for example exposure in different distances from ground etc.

As an example for the vertical radon distribution in outside air during July and August 1983 a vertical profile of the radon concentration has been measured from 0.3 m to 15.5 m above ground (Fig. 4.5). The plotted radon concentrations are mean values and standard deviations of four corresponding doseimeters. A decrease of the integrated radon concentration from 0.3 m to 3 m by a factor of 4 was found.

In consequence it has been decided to separate the outdoor measurements from those indoors. The doseimeters have been exposed standardized in the observer stations of the German Meteorological Service ('Deutscher Wetterdienst') for one year.

In contrast to the indoor measurements a radon concentration gradient has been found from the north to the south of Germany. The median concentrations for the different federal states of Germany are presented in Table 4.2. The radon concentrations outside are mainly influenced by meteorological and geological parameters. One reason besides differences in geology for the lower concentration at the coast of the North Sea is a permanent dilution with nearly radon free air from the sea.

In the south west it has been shown that the concentrations are consistent with geology. The highest concentrations have been found in areas with uranium in the ground, such as granitic areas in the Black Forest, the lowest concentrations in areas with shell lime stone.

4.2.3 Radon concentration in houses influenced by geology

Some of the measurements of the survey program in German houses have been done in the region of Freudenstadt in the Black Forest over a period of more than one year. During the exposure time in spring 1982 very high radon

Federal state	Number of measurements	Radon concentration (Bq/m ³)
Schleswig-Holstein	19	8
Hamburg	-	-
Niedersachsen	11	11
Bremen	2	12
Nordrhein-Westfalen	9	16
Hessen	44	17
Rheinland-Pfalz	15	16
Baden-Württemberg	129	23
Bayern	18	20
Saarland	2	15
Berlin	2	16

Table 4.2: Radon concentrations in outside air.

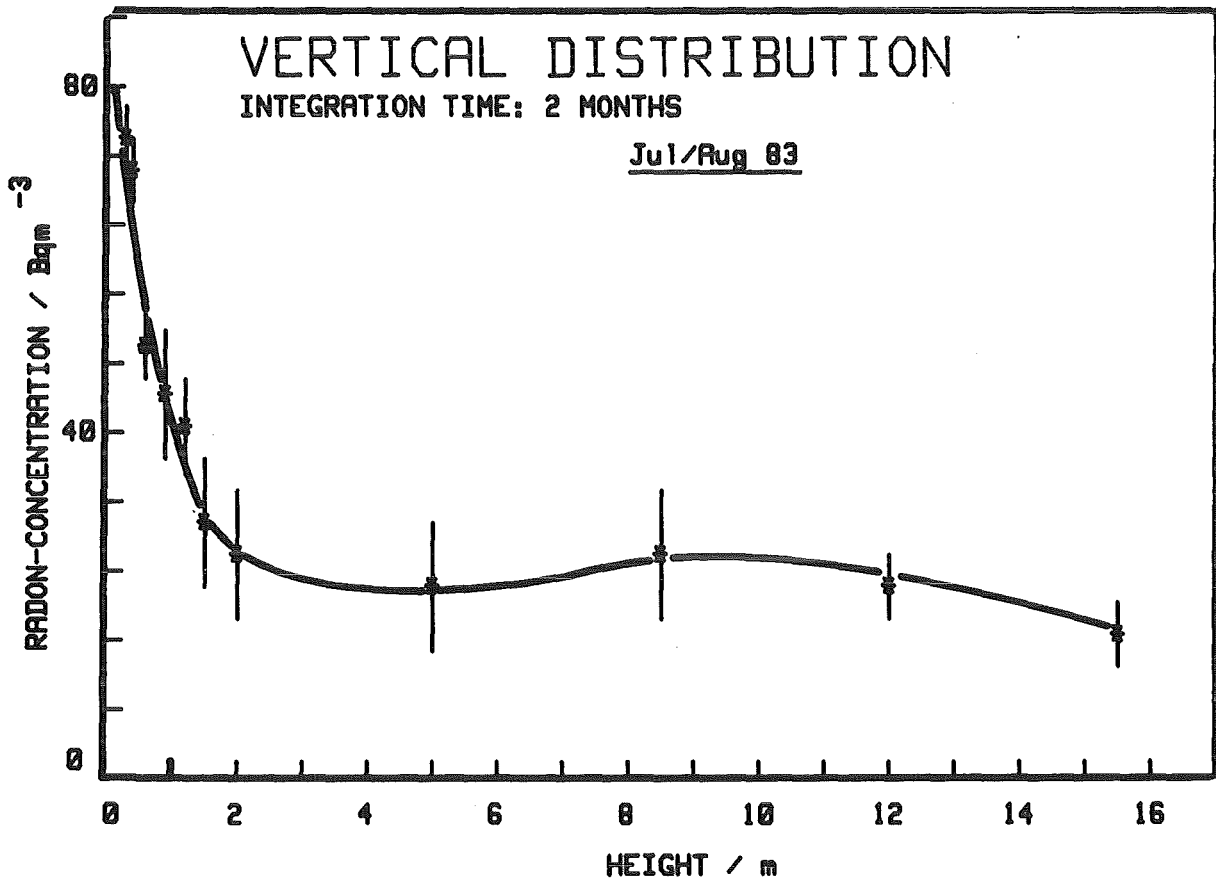


Fig. 4.5: Typical vertical profile in outside air (summer).

concentrations have been found in five houses. At the same time the radon concentrations of all other houses in that region have been more or less around the expected mean values. After that the measurements have been repeated twice resulting in normal radon concentrations. We also can be sure that no mistakes in processing the detectors have been done, because they have been processed together with the others of that region. In Fig. 4.6 a detail map shows the results of the measurements in the houses and in outside air.

All these houses have been found to be less than 100 m away from a fault, the 'Freudenstädter Verwerfung.' The only explanation can be, that during spring (period a) in 1982 there was an anomalous high radon exhalation in connection with the fault. An indication for that is also the radon concentration in outside air, which was always in the same order of magnitude as in the houses.

4.2.4 Radon concentration in houses influenced by mining activities

In a former mine building called 'Alte Schmiede' at Wittichen in the Black Forest, which was still inhabited and situated directly at the foot slope of an old cobalt/silver mine dump, the highest indoor radon concentrations were determined (Fig. 4.7) (Sc 83). In this place a more detailed study was performed, including the measurement of radon daughters and exhalation rates. The data were correlated to seasonal variations and atmospheric conditions. The correlation with the amount of rain was negative; good correlation was obtained with the number of days with rain per month (Fig. 4.8). As can be seen the concentration in this house would have gone down to 75 Bq/m^3 at about 80% rainy days per month while in extreme sunny weather periods a radon impact on the house of about $4,000 \text{ Bq/m}^3$ could have been predicted.

The highest radon concentration was measured in May 1981 with more than $5,000 \text{ Bq/m}^3$ in the living room and more than $15,000 \text{ Bq/m}^3$ in the basement.

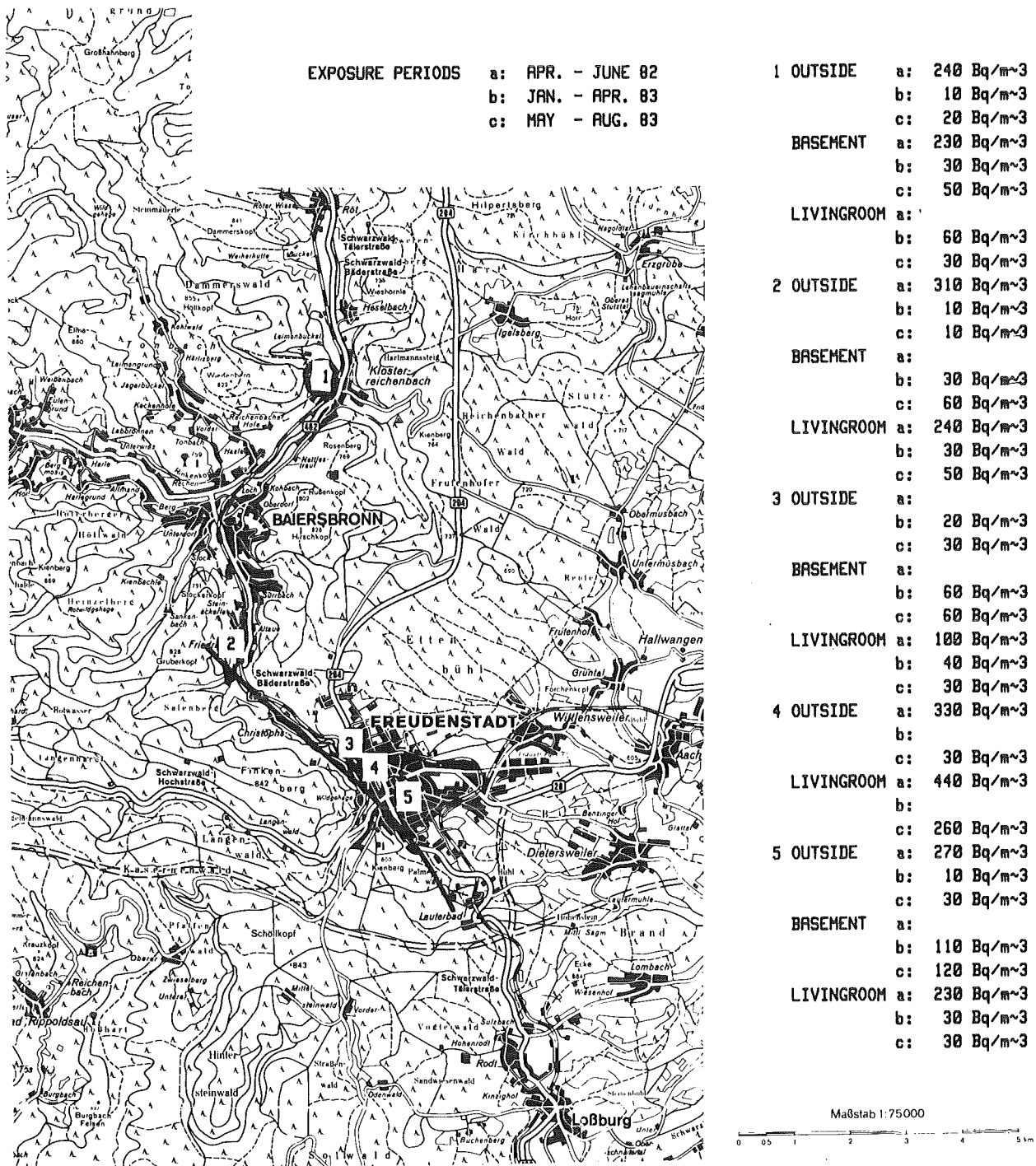


Fig. 4.6: Measurements of radon concentrations in houses located near a geological fault around Freudenstadt in the Black Forest.

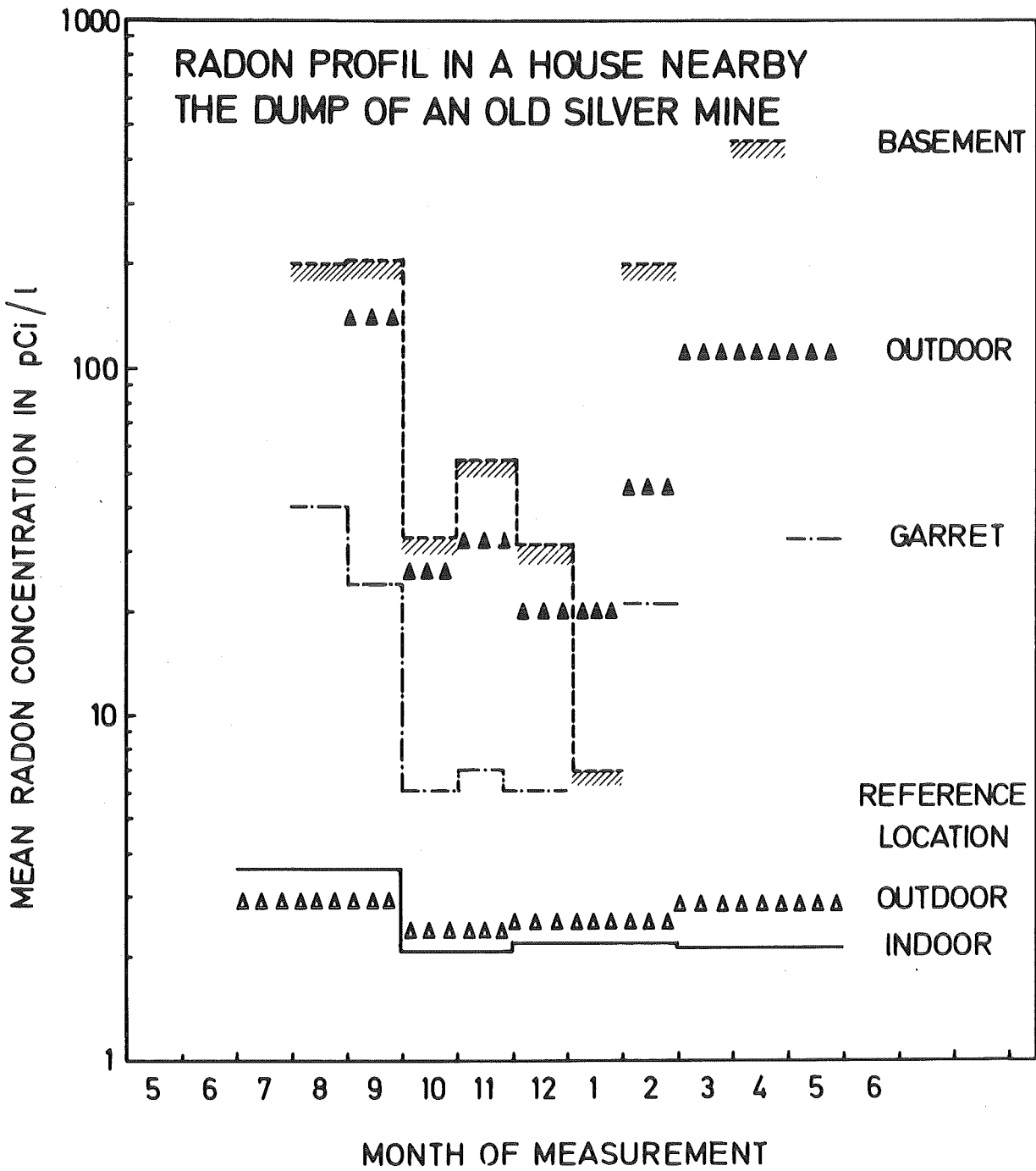


Fig. 4.7: Change in radon concentration in a house nearby a dumping ground of an old silver mine.

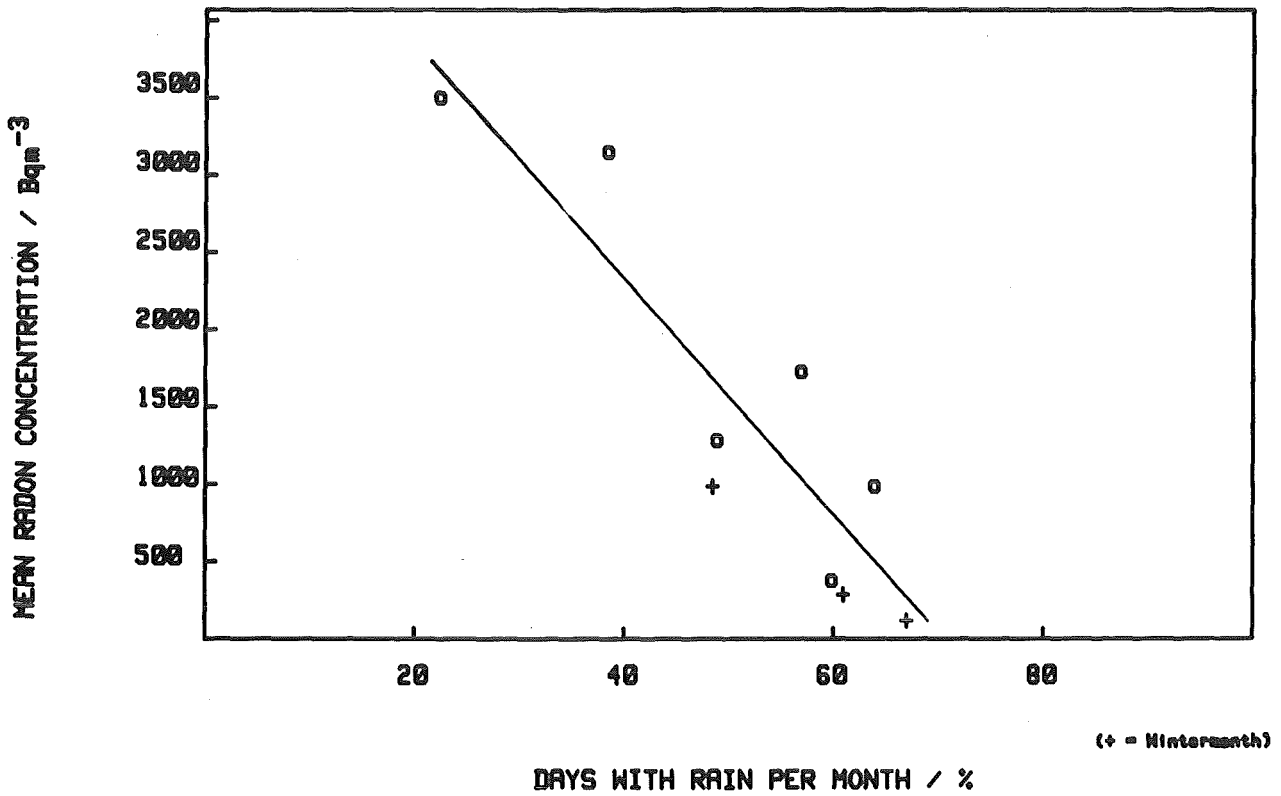


Fig. 4.8: Indoor radon concentration as a function of days with rain ('Alte Schmiede', Wittichen, 5/80 - 2/81).

As a result of realistic assumptions including the background gamma activity from the mine dump, which contains more than 2.5 Bq/g Ra-226, an effective equivalent dose exceeding 50 mSv/a for the inhabitants was calculated.

5. EXPOSURE AND DOSE ESTIMATION

5.1 Inhalation of radon and short lived decay products

Due to its inert properties radon is not chemically bounded in tissue. Therefore the uptake of radon into the body is limited by its solubility in tissue. It depends on the concentration of radon in the ambient air. With respect to the kinetics of radon transport in the body the following processes have to be distinguished (Ja 80):

- the uptake from air into blood,
- the convective transport in the blood stream,
- diffusion from blood into intracellular fluids,
- the radioactive decay during the transport.

The uptake into blood is a rapid process, which takes place in the lung. The uptake of radon from blood into body tissue happens with halflives from minutes to hours. The consequence is a nearly uniform dose distribution in the body except the lung and fat tissue due to the high solubility.

Short lived radon decay products are heavy metals. Therefore the uptake into body is different from that of the noble gas radon. They are deposited and therefore enriched in the respiratory tract. Because of the higher regional deposition, uptake from the lung to blood occurs predominantly in the pulmonary region. The fractions of deposited Po, Pb and Bi atoms taken up by the blood are given by the competing rates of radioactive decay and biological transfer represented by compartment models (Ja 80, OECD 84). The clearance models assume similar rates of biological transfer from the pulmonary region to the blood. On this basis, therefore, the fraction of inhaled Po, Pb and Bi atoms taken up by the blood depends mainly on the estimate of pulmonary deposition.

For inhalation of Rn-222 daughters Jacobi and Eisfeld (Ja 80) have shown that the dose to all tissues except the kidneys is more than two orders of magnitude lower than that absorbed by lung tissue. The kidney dose can also be neglected, however, as this is estimated to be only a few percent of lung dose.

5.2 Exposure and dose calculation

To derive from the measured radon concentrations the concentration of the short lived decay products, which are of most importance for dose estimations, assumptions have to be made for equilibrium conditions. Therefore additional measurements of the equilibrium factor (see Appendix) are necessary both for mines and for houses. A further uncertainty especially for houses is a realistic assumption for the occupancy factor. This factor describes the probability that people stay indoors or outdoors.

5.2.1 Equilibrium factor

The equilibrium factor F is defined as quotient of the equilibrium equivalent concentration of radon decay products C_e (see Appendix) and radon concentration C_{Rn} :

$$F = \frac{C_e}{C_{Rn}} \text{ and} \quad (5.1)$$

$$C_e = 0.105 C_1 + 0.516 C_2 + 0.379 C_3.$$

C_1 is the activity concentration of Po-218, C_2 that of Pb-214 and C_3 that of Bi-214.

In literature some data of measured equilibrium factors are available with reported mean values of 0.3 for underground uranium mines, 0.7 for underground non-uranium mines (UN 82) and from 0.3 to 0.7 for houses in different countries.

In Table 5.1 measured equilibrium factors in houses of different countries are presented. Unfortunately no data from South American countries is available.

The equilibrium factor in mines is mainly dependent on mine ventilation and aerosol concentration and in houses on air exchange rates and aerosol concentrations. Cigarette smoke for instance may increase the equilibrium factor in a room significantly (Fig. 5.1). The radon as well as the decay product concentration and air exchange rate was measured continuously in a test room for two weeks (Ur 84a). After 12 days several cigarettes were smoked in this room. The radon concentration decreased due to increased ventilation by opening the room. However, the concentration of decay products and therefore the equilibrium factor increased. After two days the original level was reached again.

For Germany measured equilibrium factors for underground uranium mines of 0.2 and for dwellings of 0.35 are used for estimation of mean exposure to radon and daughters.

5.2.2 Occupancy factor

Estimating radiation exposure for miners is much more easy than it is for general public. Usually exact data is available, which time each worker has spent in the mine or mill. This is not the case for members of the general public. It only can be estimated how many time on average people spend indoors. This also may be different for children, housewives and employed people. UNSCEAR suggested a factor of 0.8 indoors and 0.2 outdoors for the public (UN 84). These values are adopted in this report.

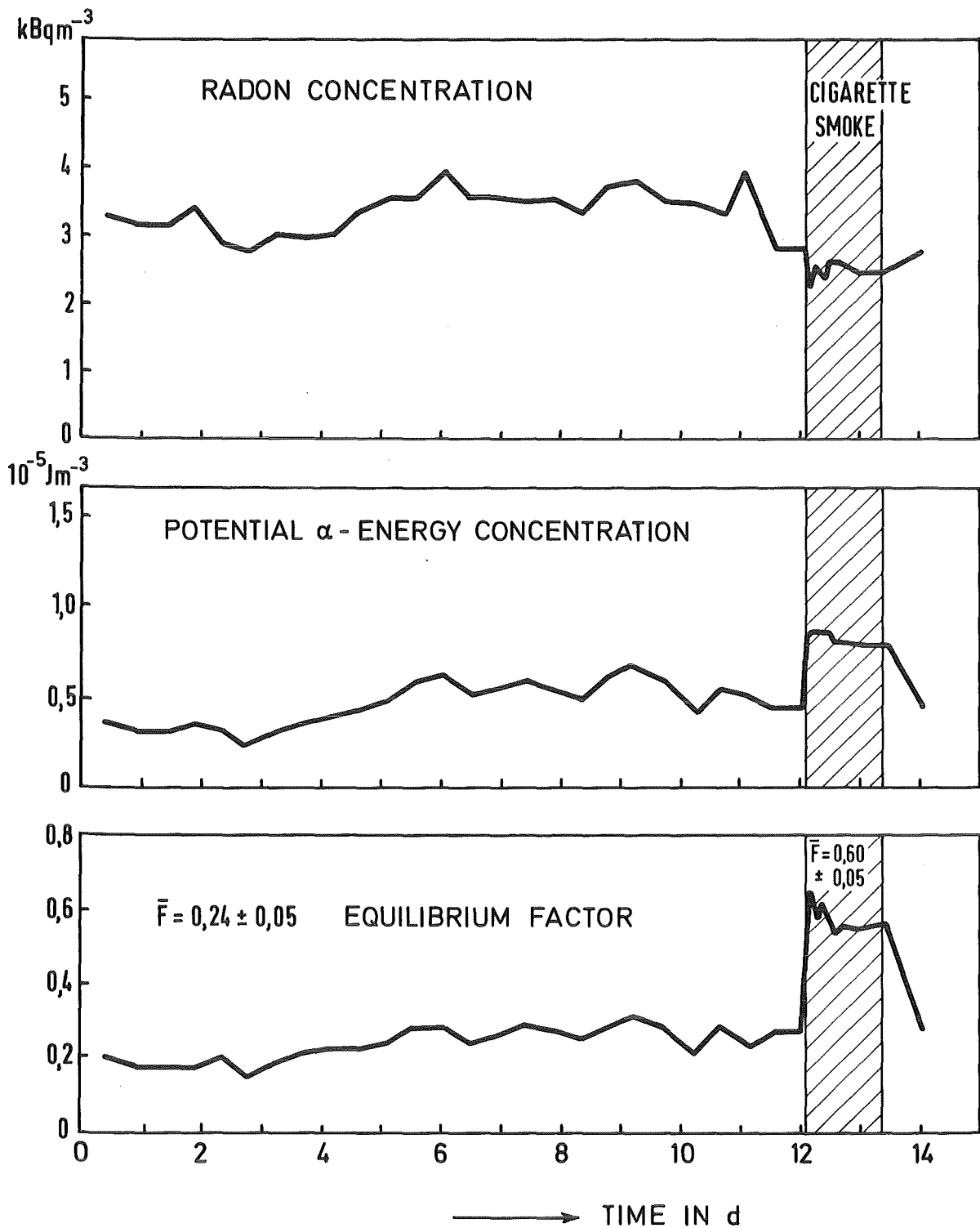


Fig. 5.1: Influence of the concentration of aerosols (cigarette smoke) in room air on the equilibrium factor.

Country	Number of houses	Equilibrium factor, median value	Range	Reference
Canada	9,118	0.52	0.2 - 0.7	Mc 80
Finland	35	0.47	0.3 - 0.6	Mä 80
Sweden	225	0.44	0.1 - 0.8	Sw 83
Norway	25	0.5	0.3 - 0.8	St 79
USA	21	0.6	0.3 - 0.8	Ge 80
Italy	?	0.6-0.7	0.4 - 0.9	Cs 84
Fed. Rep. of Germany	37	0.4		Wi 82
	130	0.3		Ke 84
	12*	0.3	0.1 - 0.7	Ur 84a

*integrated measurements up to four months.

Table 5.1: Equilibrium factors of radon decay products in houses for different countries.

5.2.3 Exposure calculation

To calculate exposure historically founded not the equilibrium equivalent radon concentration C_e but the potential alpha energy concentration C_p (unit WL 'Working Level') is used:

$$C_p \text{ (WL)} = \frac{C_e \text{ (Bq/m}^{-3}\text{)}}{3,700} \quad (5.2)$$

The exposure E_p (WLM) in units of 'Working Level Month' is the time integral of the potential alpha energy concentration assuming 170 hours for one month:

$$E_p \text{ (WLM)} = \frac{1}{170} \int_0^t C_p(t) dt = \frac{C_p t}{170} \quad (5.3)$$

In Table 5.2 the calculated mean exposures for workers in a Brazilian open pit mine and uranium processing site and in a German underground uranium mine are presented.

Assuming an equilibrium factor of 0.5 for the open pit mine and 0.2 for the underground mine the annual exposure to radon daughters in the open pit mine is about thirty times lower than that in the underground mine and is in the same order of magnitude as the exposures of the public in dwellings (Table 5.3).

The exposure calculated from the median value of the measured log-normal distributed radon concentrations in German houses cannot be compared with those of the so far small Brazilian pilot study. Comparable are measurements in two cities at the seashore resulting in the same mean exposure for the people in houses of about 0.1 WLM/a. Comparable are also those exposures derived from measurements in towns or regions near to uranium mines. These are Poços de Caldas, Andradas and Caldas in Brazil and the German Regierungsbezirk Oberfranken. The exposures found in those Brazilian towns are several times higher than those in Oberfranken. One reason for that could be

	Exposure to radon decay products (mean value) WLM
<u>BRAZIL*</u>	
Open pit mine	0.25
Milling area	0.40
Chemical uranium processing	0.09
<u>GERMANY**</u>	
Underground mine	about 6

*200 working days, 8 hours each, F = 0.5.

**dose records for each miner.

Table 5.2: Exposure to radon daughters in uranium and processing facilities.

	Number of measurements	Exposure to radon decay products, mean / median value WLM/a
<u>BRAZIL</u> (F = 0.5)		
Rio de Janeiro	104	0.13
Andradas	76	0.46
Caldas	72	0.29
Poços de Caldas	68	0.64
<u>GERMANY</u>		
Hamburg	160	0.11
Reg. Bez. Oberfranken	122	0.21
Reg. Bez. Koblenz	134	0.25
National survey	5,970	0.14

Table 5.3: Annual exposure to radon decay products in houses.

that the German measurements are spread over a bigger area and therefore not all measurements have been done in direct neighborhood of the mine. In Germany the highest exposure to radon daughters was found in a volcanic region, Regierungsbezirk Koblenz, not affected by mining or milling activities.

5.3 Dose estimation

To convert exposure to dose several theoretical models are available. These models were recently summarized by an expert group of the OECD/NEA in a special report (OECD 84). In Table 5.4 the proposed dose conversion factors for occupational and non-occupational exposure are presented.

The application of these conversion factors to Table 5.2 and Table 5.3 results in the mean effective equivalent doses presented in Table 5.5 for miners and in Table 5.6 for the general public in houses.

	Breathing rate m^3/h	Effective dose equivalent H_E	
		$\text{Sv}/\text{J h m}^{-3}$	mSv/WLM
Occupational exposure: underground and open pits	1.2	2.4	8.5
Non-occupational exposure: indoors	0.75	1.5	5.5

Table 5.4: Dose conversion factors for inhaled radon decay products (OECD 84).

	Mean effective equivalent dose mSv/a
<u>BRAZIL</u>	
Open pit mine	2.1
Milling area	3.4
Chemical ore processing	0.8
<u>GERMANY</u>	
Underground mine	about 51

Table 5.5: Effective equivalent dose for miners due to inhalation of short lived radon decay products.

	Mean effective equivalent dose* mSv/a
<u>BRAZIL</u>	
Rio de Janeiro	0.72
Andradas	2.53
Caldas	1.60
Poços de Caldas	3.52
<u>GERMANY</u>	
Hamburg	0.61
Reg. Bez. Oberfranken	1.16
Reg. Bez. Koblenz	1.38
National Survey	0.77

*exposure outdoors not included.

Table 5.6: Effective equivalent dose for the general public due to the inhalation of radon decay products in houses.

6. REFERENCES

- (Ch 78) Chapuis, A. M., et al.
Individual dosimeter for radon and daughters. OECD Specialist Meeting on Radon Monitoring, Paris, France, Nov. 1978.
- (Ge 80) George, A. C., et al.
The distribution of ambient radon and radon daughters in residential buildings in the New Jersey - New York area. Nat. Rad. Env. III, CONF-780422, p. 1272-1292.
- (Fl 69) Fleischer, R. L., Price, P. B., Woods, R. T.
Nuclear particle track identification in inorganic solids. Phys. Rev. 88, 1969, p. 563-567.
- (Fl 75) Fleischer, R. L., Price, P. B., Walker, R. M.
Nuclear tracks in solids. University of California Press, Berkeley, USA, 1975.
- (Ja 80) Jacobi, W., Eisfeld, K.
Dose to tissues and effective dose equivalent by inhalation of Rn-222, Rn-220 and their short lived daughters. GSF-report S-626, 1980.
- (Ke 84) Keller, G., Folkerts, K. H.
Radon concentrations and decay product equilibrium in dwellings and in open air. Health Physics, in press.
- (Mä 80) Mäkeläinen, I.
Preliminary survey of radon in Finnish dwellings. Meeting of the Nordic Society for Radiation Protection, Galo, Norway, 1980.
- (Mc 80) McGregor et al.
Background concentrations of radon and daughters in Canadian homes. Health Physics, Vol. 39, 1980, p. 285-289.

- (OECD 83) OECD/NEA report
Dosimetry aspects of exposure to radon and thoron daughter products. OECD, Paris, 1983.
- (Sa 74) Sayed, A. M., Piesch, E.
Study of the latent fading of NTA film and track etching detectors at various temperatures and humidities. KfK-report 2032, 1974.
- (Sc 83) Schmitz, J., Urban, M.
Mine dumps as a source of radon impact on buildings. Rad. Prot. Dos., Vol. 7, 1984, p. 63-68.
- (Sc 84) Sciocchetti, G., et al.
Indoor measurements of natural radioactivity in Italy. Rad. Prot. Dos., Vol. 7, 1984, p. 347-351.
- (To 70) Tommassino, L.
Electrochemical etching of damaged track detectors by HV pulse and sinusoidal wave form. Internal Report CNEN, Cassaccia, Roma, Italy, 1970.
- (To 81) Tommassino, L.
Electrochemical etching, mechanisms. Nucl. Tracks, Vol. 4, 1981, p. 191-196.
- (UN 82) United Nations Scientific Committee on the Effects of Atomic Radiation, Ionizing Radiation: Sources and Biological Effects. United Nations, New York, 1982.
- (Ur 81) Urban, M., Piesch, E.
Low level environmental radon dosimetry with a passive etch device. Rad. Prot. Dos., Vol. 1, 1981, p. 97-110.

- (Ur 83) Urban, M., Burgkhardt, B., Piesch, E.
Temperature and humidity dependent fading of neutron induced recoil and alpha-particle tracks in MAKROFOL. Proc. 12th Int. Conf. on Solid State Nuclear Track Detectors, Sept. 4-10, 1983, Acapulco, Mexico.
- (Ur 84a) Urban, M.
Dosisbestimmung durch gleichzeitiges Messen der Radon-/Thoronkonzentration und der Gleichgewichtsfaktoren in Luft mit Hilfe eines passiven Dosimeters. KfK-report 3726, 1984.
- (Ur 84b) Urban, M., Schmitz, J.
Applications of passive radon dosimeters in mining areas. Int. Conf. on Occupational Radiation Safety in Mining, Toronto, Canada, Oct. 14-18, 1984.
- (Wi 82) Wicke, A., Porstendörfer, J.
Radon daughter equilibrium in dwellings. Int. Conf. on Nat. Rad. Env., Bombay, India, Jan. 1981.
- (Wi 83) Wicke, A.
Methoden zur Messung von Radon, Thoron und seinen kurzlebigen Zerfallsprodukten in der Luft. Vortrag 5. Fachgespräch 'Überwachung der Umweltradioaktivität', 22.-24. März 1983, Kernforschungszentrum Karlsruhe.
- (Wi 84) Wicke, A., Urban, M., Kiefer, H.
Radon concentration levels in homes in the Federal Republic of Germany. 6th Int. IRPA Congress, Berlin, Germany, May 7-12, 1984.

7. APPENDIX

This appendix on special quantities and units is taken from the OECD/NEA report on radon dosimetry (OECD 83).

(1) Radioactive decay properties

Radon gas (^{222}Rn) is formed by the decay of ^{226}Ra ($T_R = 1600$ y) in the ^{238}U -decay series. Thoron gas (^{220}Rn) is a radionuclide in the ^{232}Th -decay series and is formed by decay of ^{224}Ra ($T_R = 3.64$ d). Radon has a radioactive half-life (T_R) of 3.823 d and thoron 55 s. The main radioactive properties of the chains of nuclides resulting from decay of radon and thoron are given in Tables A.1 and A.2, respectively. The radioactive half-life (T_R), decay constant (λ_R), the principal energy emissions and their relative intensities are here reproduced from the data of UNSCEAR (1977).

Table A.1

MAIN RADIOACTIVE DECAY PROPERTIES OF ^{222}Rn AND ITS SHORT-LIVED DAUGHTERS (FROM UN 77)¹

Radionuclide decay chain	T_R	λ_R (h^{-1})	Main energies (in MeV) and intensities		
			α	β	γ
$^{222}\text{Rn}(\text{Rn})$	3.823 d	$7.55 \cdot 10^{-3}$	5.49 (100%)	-	0.51 (0.07%)
↓ α					
$^{218}\text{Po}(\text{RaA})$	3.05 min	13.6	6.00 (~100%)	0.33 (~0.019%)	-
↓ α					
$^{214}\text{Pb}(\text{RaB})$	26.8 min	1.55	-	0.65 (50%) 0.71 (40%) 0.98 (6%)	0.295 (19%) 0.352 (36%)
↓ β, γ					
$^{214}\text{Bi}(\text{RaC})$	19.7 min	2.11	5.45 (0.012%) 5.51 (0.008%)	1.0 (23%) 1.51 (40%) 3.26 (19%)	0.609 (47%) 1.12 (17%) 1.76 (17%)
↓ β, γ					
$^{214}\text{Po}(\text{RaC}')$	164 μs	$1.52 \cdot 10^7$	7.69 (100%)	-	0.799 (0.014%)
↓ α					

¹The branchings from ^{218}Po and ^{214}Po can be neglected, due to their low yield of 0.02%

Table A.2

MAIN RADIOACTIVE DECAY PROPERTIES OF ^{220}Rn AND ITS DAUGHTERS (FROM UN 77)

Radionuclide decay chain	T_r	λ_T (h^{-1})	Main energies (in MeV) and intensities		
			α	β	γ
$^{220}\text{Rn}(\text{Tn})$	55 s	45.4	6.29 (100%)	-	0.55 (0.07%)
\downarrow α					
$^{216}\text{Po}(\text{ThA})$	0.15 s	$1.58 \cdot 10^4$	6.78 (100%)	-	-
\downarrow α					
$^{212}\text{Pb}(\text{ThB})$	10.64 h	0.06514	-	0.346 (81%) 0.586 (14%)	0.239 (47%) 0.300 (3.2%)
\downarrow β, γ					
$^{212}\text{Bi}(\text{ThC})$	60.6 min	0.686	6.05 (25%) 6.09 (10%)	1.55 (5%) 2.26 (55%)	0.040 (2%) 0.727 (7%)
\swarrow β, γ (64%)					
\searrow α (36%)					
$^{212}\text{Po}(\text{ThC}')$	304 ns	$8.21 \cdot 10^9$	8.78 (100%)	-	-
\swarrow α					
$^{208}\text{Tl}(\text{ThC}''')$	3.10 min	13.4	-	1.28 (25%) 1.52 (21%) 1.80 (50%)	0.511 (23%) 0.583 (86%) 0.860 (12%) 2.614 (100%)
\swarrow β, γ					

(2) Potential α -energy

The potential α -energy of an atom, ϵ_p , is the total α -energy emitted during decay of this atom through the decay chain to ^{210}Pb (RaD) or ^{208}Pb (ThD), respectively. The total potential α -energy per Bq of activity of a radionuclide is given by ϵ_p/λ_r , where the decay constant λ_r is expressed in s^{-1} . Values of ϵ_p and ϵ_p/λ_r for the radon and thoron decay chains are given in Table A.3.

Table A.3

POTENTIAL α -ENERGY PER ATOM AND PER Bq

Radionuclide	Potential α -energy			
	per atom (ϵ_p)		per Bq (ϵ_p/λ_p)	
	in MeV	in 10^{12} J	in MeV	in 10^{-10} J
$^{222}\text{Rn}(\text{Rn})$	19.2	3.07	$9.15 \cdot 10^6$	14 700
$^{218}\text{Po}(\text{RaA})$	13.7	2.19	3 620	5.79
$^{214}\text{Pb}(\text{RaB})$	7.69	1.23	17 800	28.6
$^{214}\text{Bi}(\text{RaC})$	7.69	1.23	13 100	21.0
$^{214}\text{Po}(\text{RaC}')$	7.69	1.23	$2.0 \cdot 10^{-3}$	$3.0 \cdot 10^{-6}$
$^{220}\text{Rn}(\text{Tn})$	20.9	3.34	1 660	2.65
$^{216}\text{Po}(\text{ThA})$	14.6	2.34	3.32	$5.32 \cdot 10^{-3}$
$^{212}\text{Pb}(\text{ThB})$	7.80	1.25	$4.31 \cdot 10^5$	691
$^{212}\text{Bi}(\text{ThC})$	7.80	1.25	$4.09 \cdot 10^4$	65.6
$^{212}\text{Po}(\text{ThC}')$	8.78	1.41	$3.85 \cdot 10^{-6}$	$6.2 \cdot 10^{-9}$

(3) Potential α -energy concentration in air

The potential α -energy concentration of any mixture of short-lived ^{222}Rn - or ^{220}Rn -daughters is the sum of the potential α -energy of all daughter atoms present per unit volume of air. This quantity can be expressed in SI-units:

$$1 \text{ J m}^{-3} = 6.24 \times 10^{12} \text{ MeV m}^{-3} = 6.24 \times 10^9 \text{ MeV l}^{-1}$$

The special unit 1 WL (Working Level) is often used for this quantity:

$$1 \text{ WL} = 1.3 \times 10^5 \text{ MeV l}^{-1} = 2.08 \times 10^{-5} \text{ J m}^{-3}$$

1 WL corresponds approximately to the potential α -energy concentration of short-lived ^{222}Rn -daughters in air which are in radioactive equilibrium with a ^{222}Rn -activity concentration of $100 \text{ pCi l}^{-1} = 3.7 \text{ Bq l}^{-1} = 3700 \text{ Bq m}^{-3}$.

For ^{220}Rn -daughters in radioactive equilibrium with ^{220}Rn , 1 WL corresponds to a ^{220}Rn -concentration of $7.43 \text{ pCi l}^{-1} = 275 \text{ Bq m}^{-3}$.

In Table A.4 the conversion factors between activity concentration (in Bq m^{-3}) and potential α -energy concentration are listed for the short-lived daughter nuclides of ^{222}Rn and ^{220}Rn .

Table A.4

POTENTIAL α -ENERGY CONCENTRATION PER Bq m⁻³

Radionuclide	MeV l ⁻¹	10 ⁻¹⁰ J m ⁻³	10 ⁻⁶ WL
²¹⁸ Po(RaA)	3.62	5.79	27.8
²¹⁴ Pb(RaB)	17.8	28.6	137
²¹⁴ Bi(RaC)	13.1	21.0	101
²¹⁴ Po(RaC')	2.0 10 ⁻⁶	3.0 10 ⁻⁶	1.6 10 ⁻⁵
²¹⁶ Po(ThA)	3.32 10 ⁻³	5.32 10 ⁻³	0.0256
²¹² Pb(ThB)	431	691	3 320
²¹² Bi(ThC)	40.9	65.6	315
²¹² Po(ThC')	3.85 10 ⁻⁹	6.2 10 ⁻⁹	3.0 10 ⁻⁸

(4) Equilibrium equivalent radon concentration (EC_{Rn}) and equilibrium factor (F)

The EC_{Rn} of a non-equilibrium mixture of short-lived Rn-daughters in air is that activity concentration of Rn in radioactive equilibrium with its short-lived daughters that has the same potential α -energy concentration, c_p . Therefore for ²²²Rn and its daughters:

$$\begin{aligned} EC_{Rn} \text{ (Bq m}^{-3}\text{)} &= 2.85 \times 10^{-2} c_p \text{ (MeV l}^{-1}\text{)} \\ &= 1.78 \times 10^8 c_p \text{ (J m}^{-3}\text{)} \\ &= 3700 c_p \text{ (WL)} \end{aligned}$$

$$[\text{ie, } EC_{Rn} \text{ (pCi l}^{-1}\text{)} = 100 c_p \text{ (WL)}]$$

and for ²²⁰Rn and its daughters:

$$\begin{aligned} EC_{Tn} \text{ (Bq m}^{-3}\text{)} &= 2.12 \times 10^{-3} c_p \text{ (MeV l}^{-1}\text{)} \\ &= 1.32 \times 10^7 c_p \text{ (J m}^{-3}\text{)} \\ &= 275 c_p \text{ (WL)} \end{aligned}$$

The "equilibrium factor", F, with respect to potential α -energy is defined as the ratio of the EC_{Rn} to the actual activity concentration, c_{Rn} , of radon in air:

$$F = \frac{EC_{Rn}}{c_{Rn}}$$

(5) Activity and potential α -energy exposure (E)

The "activity exposure" of an individual to ²²²Rn or ²²⁰Rn is the time-integral over the activity concentration of ²²²Rn or ²²⁰Rn, respectively, to which the individual is exposed during a definite period of time. Its unit is for example Bq h m⁻³.

The equivalent quantity for the short-lived ^{222}Rn - or ^{220}Rn -daughters is the "potential α -energy exposure" of an individual during a definite period of time. This quantity can be expressed in the units

$$1 \text{ J h m}^{-3} = 6.24 \times 10^9 \text{ MeV h l}^{-1} = 4.80 \times 10^4 \text{ WL h}$$

$$1 \text{ WL h} = 1.3 \times 10^5 \text{ MeV h l}^{-1} = 2.08 \times 10^{-5} \text{ J h m}^{-3}$$

The potential α -energy exposure of miners is often expressed in the unit 1 WLM (Working Level Month). 1 WLM corresponds to an exposure of 1 WL during the reference working period of 1 month (2000 working hours per year/12 months \approx 170 h):

$$1 \text{ WLM} = 170 \text{ WL h} = 2.2 \times 10^7 \text{ MeV h l}^{-1} = 3.5 \times 10^{-3} \text{ J h m}^{-3}$$

$$1 \text{ J h m}^{-3} = 285 \text{ WLM}$$

A potential α -energy exposure of 1 WLM ^{222}Rn -daughters is associated with an EC_{Rn} activity exposure of $6.3 \times 10^5 \text{ Bq h m}^{-3}$.

(6) Activity and potential α -energy intake by inhalation (I)

The "potential α -energy intake" of an individual by inhalation of radon-daughters is the inhaled potential α -energy of the daughter mixture during a definite period of time. If \bar{V} is the mean breathing rate during this period, the potential α -energy intake, I_p , is related to the potential α -energy exposure, E_p , by:

$$I_p = \bar{V} \cdot E_p$$

For the reference worker ($\bar{V} = 1.2 \text{ m}^3 \text{ h}^{-1}$) the following conversion factors apply:

Exposure, E_p \longrightarrow Intake, I_p

1 MeV h m^{-3} corresponds to $1.92 \times 10^{-13} \text{ J}$

1 WL h corresponds to $2.5 \times 10^{-5} \text{ J}$

1 WLM corresponds to $4.2 \times 10^{-3} \text{ J}$

1 J h m^{-3} corresponds to 1.2 J

For the reference adult exposed in a house ($\bar{V} = 0.75 \text{ m}^3 \text{ h}^{-1}$) the following conversion factors apply:

Exposure, E_p \longrightarrow Intake, I_p

1 MeV h m^{-3} corresponds to $1.2 \times 10^{-13} \text{ J}$

1 WL h corresponds to $1.56 \times 10^{-5} \text{ J}$

1 WLM corresponds to $2.63 \times 10^{-3} \text{ J}$

1 J h m^{-3} corresponds to 0.75 J

"Activity intake" by inhalation is the inhaled activity of a radionuclide during a definite period of time. Intake of potential α -energy, I_p , is related to intake of activity, I_a , by:

$$I_p = \left(\frac{E_p}{\lambda_r} \right) \cdot I_a$$

The conversion factor E_p/λ_r is the potential α -energy per unit of activity of the daughter nuclide being considered. The following rounded values of the ratio (I_p/I_a) and (I_a/I_p) are recommended for practical purposes (ICRP, 1981).

Table A.5

CONVERSION FACTORS BETWEEN ACTIVITY INTAKE (I_a) AND POTENTIAL α -ENERGY INTAKE (I_p) FOR ^{222}Rn - AND ^{220}Rn -DAUGHTERS

Radionuclide	$I_p (10^{-10} \text{ J})$	$I_a (10^8 \text{ Bq})$
	$I_a (\text{Bq})$	$I_p (\text{J})$
$^{218}\text{Po}(\text{RaA})$	5.8	17.2
$^{214}\text{Pb}(\text{RaB})$	28.6	3.50
$^{214}\text{Bi}(\text{RaC})$	21.0	4.76
$^{216}\text{Po}(\text{ThA})$	0.0053	18 900
$^{212}\text{Pb}(\text{ThB})$	691	0.145
$^{212}\text{Bi}(\text{ThC})$	65.6	1.52